

การตรวจสอบลักษณะเฉพาะของ Ce-TZP ที่ผ่านการแอนนัลในสูญญากาศ



นาย ปรีวิทย์ นันทสันติ

สถาบันวิทยบริการ

จุฬาลงกรณ์มหาวิทยาลัย

วิทยานิพนธ์นี้เป็นส่วนหนึ่งของการศึกษาตามหลักสูตรปริญญาวิทยาศาสตรมหาบัณฑิต

สาขาวิชาเทคโนโลยีเซรามิก ภาควิชาวัสดุศาสตร์

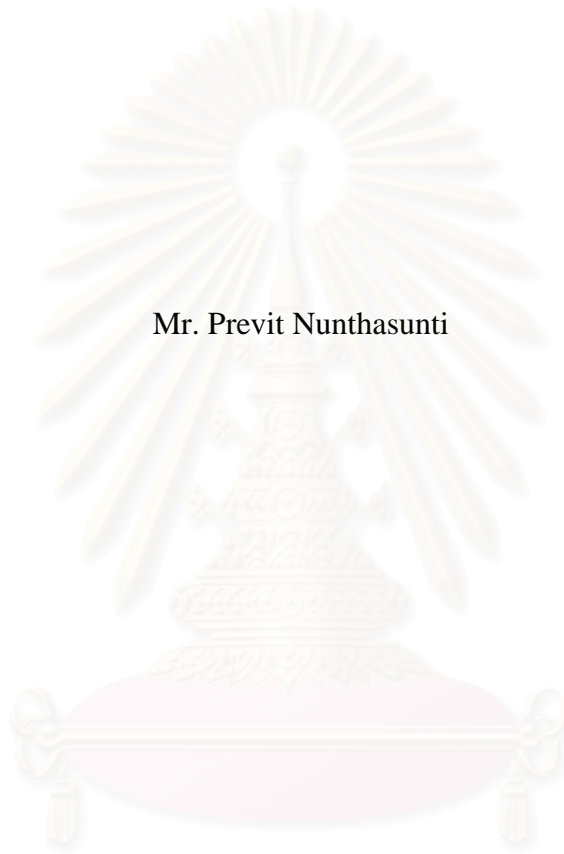
คณะวิทยาศาสตร์ จุฬาลงกรณ์มหาวิทยาลัย

ปีการศึกษา 2547

ISBN 974-17-6406-5

ลิขสิทธิ์ของจุฬาลงกรณ์มหาวิทยาลัย

CHARACTERIZATION OF Ce-TZP ANNEALED IN VACUUM ATMOSPHERE



Mr. Previt Nunthasunti

สถาบันวิทยบริการ
A Thesis Submitted in Partial Fulfillment of the Requirements
for the Degree of Master of Science in Ceramic Technology

Department of Materials Science

Faculty of Science

Chulalongkorn University

Academic Year 2004

ISBN 974-17-6406-5

Thesis Title Characterization of Ce-TZP annealed in vacuum atmosphere
By Previt Nunthasunti
Field of study Ceramic Technology
Thesis Advisor Professor Shigetaka Wada, Ph.D.
Thesis Co-advisor Associate Professor Supatra Jinawath, Ph.D.

Accepted by the Faculty of Science, Chulalongkorn University in Partial
Fulfillment of the Requirements for the Master's Degree

..... Dean of the Faculty of Science
(Professor Piamsak Menasveta, Ph.D.)

THESIS COMMITTEE

..... Chairman
(Associate Professor Saowaroj Chuayjuljit)

..... Thesis Advisor
(Professor Shigetaka Wada, Ph.D.)

..... Thesis Co-advisor
(Associate Professor Supatra Jinawath, Ph.D.)

..... Member
(Sirithan Jiemsirilerts, Ph.D.)

..... Member
(Dujreutai Pongkao, Ph.D.)

ปรีวิทย์ นันทสันติ : การตรวจสอบลักษณะเฉพาะของ Ce-TZP ที่ผ่านการแอนนีสในสุญญากาศ (CHARACTERIZATION OF Ce-TZP ANNEALED IN VACUUM ATMOSPHERE) อ. ที่ปรึกษา: ศ.ดร. ชิกเตกอะวาดะ, อ.ที่ปรึกษาร่วม: รศ.ดร. สุพัตรา จินาวัฒน์, 48 หน้า. ISBN 974-17-6406-5.

Ce-TZP เป็นวัสดุที่น่าสนใจในงานเชิงวิศวกรรมเนื่องจากสมบัติเชิงกลที่โดดเด่น นอกจากนั้นสมบัติเชิงกลของ Ce-TZP สามารถปรับปรุงได้โดยกระบวนการ heat treatment ในบรรยากาศรีดักชัน ในการทดลองนี้นำชิ้นงานมาเผาที่อุณหภูมิต่างๆกันเพื่อต้องการความหนาแน่นที่มากที่สุด หลังจากนั้นนำชิ้นงานมาทำการ heat treatment ที่อุณหภูมิ 1100 ถึง 1400°C ในบรรยากาศสุญญากาศในเตาเผาอุณหภูมิสูง โดยทำการศึกษาสมบัติต่างๆของชิ้นงานทั้งก่อนและหลังทำ heat treatment หลังจากการทำ heat treatment สีของชิ้นงานเปลี่ยนจากสีเหลืองอ่อนไปเป็นสีน้ำตาลเข้มเนื่องจากบรรยากาศรีดักชันรีดิวซ์ Ce^{4+} เป็น Ce^{3+} น้ำหนักของชิ้นงานหลังทำการ heat treatment ไม่เปลี่ยนแปลงมาก (น้อยกว่า 0.02 เปอร์เซ็นต์) เฟสของชิ้นงานเมื่อทำ heat treatment ที่อุณหภูมิ 1100°C ยังคงเป็นเฟสเตตระโกนอลเหมือนชิ้นงานที่ผ่านการเผา แต่ชิ้นงานที่ทำ heat treatment ที่อุณหภูมิ 1200°C เป็นเฟสโมโนคลินิกทั้งหมด ความแข็งแรงดัดของชิ้นงานหลังทำ heat treatment เพิ่มขึ้นจาก 555 เป็น 621 เมกะปาสคาล เฟสโมโนคลินิกทำให้ปริมาตรที่ผิวของชิ้นงานเพิ่มขึ้น จึงทำให้เกิด compressive layer ที่ผิว จึงทำให้ความแข็งแรงดัดมีค่าสูงขึ้น ในการหาค่าความแข็งของวัสดุที่แรงกด 10 ถึง 50 กิโลกรัม พบว่าไม่มีรอยแตกออกจากมุมของรอยกด และพบว่ากระบวนการ heat treatment ไม่มีผลต่อความแข็งของวัสดุ

สถาบันวิทยบริการ
จุฬาลงกรณ์มหาวิทยาลัย

ภาควิชาวัสดุศาสตร์
สาขาวิชาเทคโนโลยีเซรามิก
ปีการศึกษา 2547

ลายมือชื่อนิสิต
ลายมือชื่ออาจารย์ที่ปรึกษา.....
ลายมือชื่ออาจารย์ที่ปรึกษาร่วม

4572371223 : MAJOR CERAMIC TECHNOLOGY

KEY WORD : ZIRCONIA / CERIA / VACUUM / HARDNESS / STRENGTH

PREVIT NUNTHASUNTI: CHARACTERIZATION OF Ce-TZP ANNEALED IN VACUUM ATMOSPHERE. THESIS ADVISOR: PROF. SHIGETAKA WADA, Ph.D., THESIS CO-ADVISOR: ASSOC. PROF. SUPATRA JINAWATH, Ph.D., 48 pp. ISBN 974-17-6406-5.

12 mol% CeO₂-doped tetragonal zirconia polycrystals (12Ce-TZP) has been considered as a candidate material for engineering application because of its outstanding mechanical properties. Furthermore, mechanical properties of Ce-TZP can be improved by heat treatment in reduction atmosphere. In this experiment, specimens were sintered at various temperatures to reach full density. After that, specimens were heat treated by annealing at 1100 to 1400°C in vacuum in a high temperature furnace (hot pressed furnace). The mechanical properties of specimens before and after heat treatment were studied. After annealing, the color of specimen changed from yellowish white to dark brown since the reduction atmosphere reduced Ce⁴⁺ to Ce³⁺. However, the weight loss after heat treatment was too small (less than 0.02%). The phase of specimen annealed at 1100°C remained tetragonal which was the same as the sintered one. On the other hand, specimens after annealing at 1200°C showed pure monoclinic phase. The bending strength of this specimen increased from 555 to 621 MPa. The monoclinic phase on the surface of specimen increased the volume of the specimen surface hence induced the compressive layer on the surface. In indentation loading of 10 to 50 kgf, no cracks occurred from the indent corners. Hardness before and after annealing did not change so much in every heat treatment condition.

สถาบันวิทยบริการ
จุฬาลงกรณ์มหาวิทยาลัย

Department Materials Science

Field of study Ceramic Technology

Academic year 2004

Student's signature

Advisor's signature

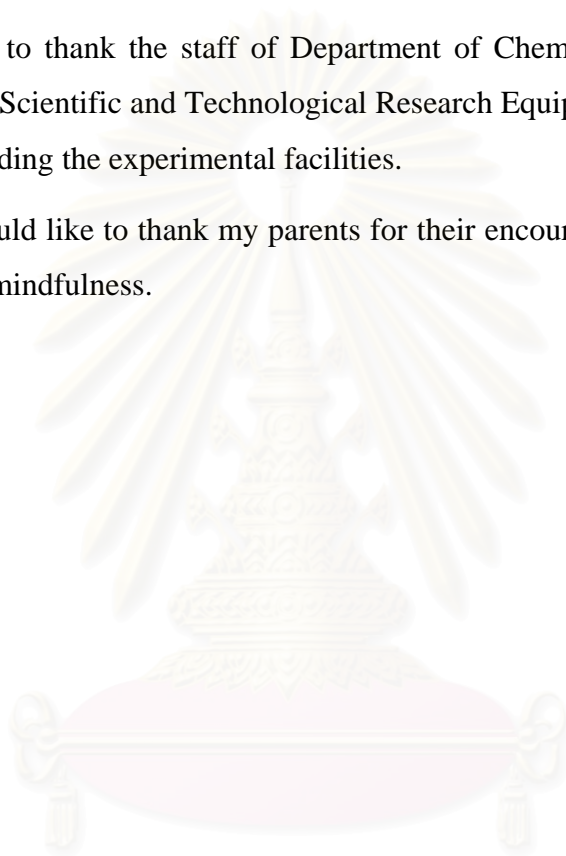
Co-advisor's signature

Acknowledgements

I would like to express my gratitude to my advisor, Professor Dr. Shigetaka Wada, for his guidance, encouragement and for all which I have learnt from him throughout this research. I would like to extend my gratitude to my co-advisor, Asst. Professor Dr. Supatra Jinawath, for her kindness understanding and invaluable suggestions.

I would like to thank the staff of Department of Chemical Engineering, Faculty of Engineering and the Scientific and Technological Research Equipment Center, Chulalongkorn University, for providing the experimental facilities.

Finally, I would like to thank my parents for their encouragement, my friends and my colleagues for their mindfulness.



สถาบันวิทยบริการ
จุฬาลงกรณ์มหาวิทยาลัย

CONTENTS

	Page
Abstract (Thai).....	iv
Abstract (English).....	v
Acknowledgements	vi
Contents	vii
List of Tables	ix
List of Figures.....	x
CHAPTER 1 INTRODUCTION.....	1
CHAPTER 2 LITERATURE REVIEW.....	2
2.1 Introduction to ZrO ₂	2
2.1.1 Polymorphism.....	2
2.1.2 Stabilization	2
2.1.3 Transformation toughening	3
2.2 Introduction to Ce-TZP	4
2.2.1 Literature review of Ce-TZP	4
2.2.2 Mechanical properties and applications.....	5
2.2.3 Literature review of heat-treatment in reduction atmosphere.....	5
CHAPTER 3 EXPERIMENTAL PROCEDURE	11
3.1 Experimental procedure	11
3.2 Raw material	12
3.3 Sample preparation	13
3.4 Characterization	13
3.4.1 Density.....	13
3.4.2 Bending strength.....	13
3.4.3 Vickers hardness.....	14
3.4.4 Microstructure	15
3.4.5 Phase analysis	15
CHAPTER 4 RESULTS AND DISCUSSION	16
4.1 Raw material characterization.....	16
4.1.1 Phase analysis	16
4.2 Sintered specimen characterizations	17

CONTENTS (cont.)

	Page
4.2.1 Relative density	17
4.2.2 Average grain size	18
4.2.3 Phase analysis	19
4.3 Annealed specimen characterizations	19
4.3.1 Preliminary annealing of pellet.....	19
4.3.2 Weight loss of annealed specimens	22
4.3.3 Color of annealed specimens	23
4.3.4 Surface observation of annealed specimens	23
4.3.5 Phase analysis of annealed specimens	26
4.4 Mechanical properties	28
4.4.1 Hardness (Hv).....	28
4.4.2 Bending strength.....	30
4.5 Comparison between former papers	32
CHAPTER 5 CONCLUSION	33
CHAPTER 6 FUTURE WORK	34
REFERENCES	35
APPENDICES	37
Appendix 1 SEM micrographs of thermal and chemical etched specimens.....	38
Appendix 2 XRD patterns of preliminary annealed specimens	40
Appendix 3 Weight loss of annealed specimens.....	43
Appendix 4 Vickers hardness of annealed specimens	45
Appendix 5 Bending strength of annealed specimens	47
BIOGRAPHY	48

LIST OF TABLES

	Page
Table 2.1 Lattice parameter of ZrO_2	2
Table 2.2 Mechanical properties of Ce-TZP	5
Table 3.1 The chemical composition and other properties of CEZ-12SD powder	12
Table 3.2 The remark of annealed specimens	13
Table 4.1 Conditions of annealing and properties after annealing of the former researches and this research.....	32



สถาบันวิทยบริการ
จุฬาลงกรณ์มหาวิทยาลัย

LIST OF FIGURES

	Page
Figure 2.1 Phase diagram of $ZrO_2 - CeO_2$	4
Figure 2.2 Phase diagram of $ZrO_2 - \frac{1}{2}Ce_2O_3$	6
Figure 2.3 The Vickers indentation (load = 1000 N) in hot isostatically pressed 12Ce-TZP ...	7
Figure 2.4 Weight loss versus annealing time in reduction heat treatment in flowing hydrogen gas at 600, 700, 800 and 1000°C for 12Ce-TZP.....	8
Figure 2.5 Fracture toughness and hardness, obtained from surface indentations, after 20 min annealing in Ar (5% N_2) at different temperatures. The starting samples were sintered in air for 1 h at 1450 or 1600°C.....	9
Figure 2.6 Fracture toughness (a) and Vickers hardness (b), obtained from surface indentations, as a function of annealing time and temperature in air and Ar (5% N_2). Starting sample was sintered in air for 60 min at 1450°C	10
Figure 3.1 Flow chart of experimental procedure	11
Figure 3.2 Flow chart of characterization.....	12
Figure 4.1 XRD pattern of as-received CEZ-12SD.....	16
Figure 4.2 Relationship between relative density and sintering temperature.....	17
Figure 4.3 SEM micrograph of Ce-TZP sintered at 1450°C and thermal etched.....	18
Figure 4.4 Average grain size of Ce-TZP sintered at 1450-1550°C.....	18
Figure 4.5 X-ray diffraction patterns of the specimens sintered at 1450°C and 1550°C.....	19
Figure 4.6 Colors of specimen sintered at 1450-1550°C and annealed at 1100-1400°C with a soaking time of 30 min, top side (left) and bottom side (right).....	20
Figure 4.7 Optical micrographs of Ce-TZP sintered at 1550°C, annealed at 1300°C (a) bottom surface annealed at 1400°C (b) edge of top surface and (c) bottom surface.....	21
Figure 4.8 Relationship between weight loss and annealing time of specimens annealed at 1100 and 1200°C.....	22
Figure 4.9 Colors of specimen sintered at 1450 and 1550°C and annealed at 1100 and 1200°C with soaking time of 15, 30 and 60 min	23
Figure 4.10 SEM micrographs of specimen sintered at 1550°C and annealed in vacuum at 1100°C and soaking time (a) 15, (b) 30 and (c) 60 min and 1200°C and soaking time (d) 15, (e) 30 and (f) 60 min.....	24

LIST OF FIGURES (cont.)

	Page
Figure 4.11 EDX patterns of specimen sintered at 1550°C (a), large grain of specimen annealed specimen at 1100°C for 60 min (b), large grain (c) and small grain (d) specimen annealed at 1200°C for 60 min.....	25
Figure 4.12 XRD patterns of specimens sintered at 1550°C and annealed in vacuum at (a) 1100°C and (b) 1200°C at various soaking time.....	27
Figure 4.13 Vickers hardness of specimens sintered at 1450 and 1550°C, annealed at 1100 and 1200°C using various soaking time	29
Figure 4.14 Optical micrographs of Ce-TZP sintered at 1550°C with indentation load of 10 kg (a) and annealed at 1200°C, soaking time 15 min with indentation loading of 30 kg (b), 50 kg (c).....	30
Figure 4.15 Bending strengths of specimens sintered at 1450 and 1550°C, annealed at 1100 and 1200°C with various soaking time	31

CHAPTER 1

INTRODUCTION

Zirconia ceramics (ZrO_2) are considered as a candidate material for engineering application because of its outstanding mechanical properties. It has intrinsic physical and chemical properties, such as high hardness, good wear resistance, large elastic modulus, good chemical resistance, low thermal conductivity and high melting point that make it attractive for various engineering applications. However, the phase transformation changes phase of zirconia from tetragonal to monoclinic. It makes volume increase about 3-5% when component is cooled from sintering temperature. Then microcracks occur and mechanical properties of the component are decreased. To solve this problem, some amount of metal oxides such as CeO_2 , Y_2O_3 , MgO and CaO is added to zirconia to stabilize phase transformation.

Ceria-stabilized tetragonal zirconia polycrystals (Ce-TZP) are interesting for structural application because of their remarkable toughness. There are many reports on the processing of Ce-TZP. A large variation in toughness is reported from 5 to 16 $\text{MPa}\cdot\text{m}^{1/2}$. Although, Y_2O_3 -doped zirconia ceramic (Y-TZP) has a superior mechanical property, it shows a dramatic loss in mechanical property when it is annealed at temperatures between 100 and 300°C, due to hydrothermal aging. (1) On the other hand, this loss is not observed in Ce-TZP. Moreover, the mechanical properties of Ce-TZP, especially fracture toughness and bending strength, can be improved by heat-treatment under reduction atmosphere.

The present experiment is focused on the mechanical properties of Ce-TZP, which is sintered at 1350-1550°C and heat-treated in vacuum using various annealing temperatures and soaking times. The goal of the present research is to develop high mechanical property zirconia ceramics, especially in bending strength, and to reduce the production cost by using low-cost Ce-TZP powder.

CHAPTER 2

LITERATURE REVIEW

2.1 Introduction to ZrO₂

2.1.1 Polymorphism

Zirconium compounds are obtained from natural minerals, mainly zircon beach sands (ZrO₂·SiO₂) and baddeleyite (ZrO₂), and are composed of a small amount of hafnium oxide (HfO₂). Zirconia is in the monoclinic form at room temperature because it is stable at the lowest temperature (lower than 1170°C). Furthermore, a tetragonal structure is stable at intermediate temperature (1170-2370°C) and a cubic form is stable at the highest temperature (2370-2680°C).

Table 2.1 Lattice parameter of ZrO₂

Lattice / Crystal structure	a (Å)	b (Å)	c (Å)
Monoclinic (<i>m</i>) $\beta = 98.9^\circ$	5.156	5.191	5.304
Tetragonal (<i>t</i>)	5.094	--	5.177
Cubic (<i>c</i>)	5.124	--	--

The lattice parameters of ZrO₂ are shown in table 2.1. The tetragonal to monoclinic phase transformation occurs with the volume expansion of 3-5%. This volume expansion induces microcrack to generate and results in the decrease in the mechanical strength of zirconia.

2.1.2 Stabilization

The *t*-to-*m* transformation ZrO₂ when cooled from the fabrication temperature is the problem of ZrO₂. To solve this problem, the phase transformation in ZrO₂ has been modified by controlling the amount of metal oxide additives such as MgO, CaO, Y₂O₃ and CeO₂. By adding these modifiers, ZrO₂ is stabilized to cubic phase. However, the mechanical strength of cubic ZrO₂ is not high. Then, the two systems, tetragonal zirconia polycrystals (TZP) and partially stabilized zirconia (PSZ), have been developed commercially. The TZP is

a ZrO_2 based ceramic where the matrix grains are stabilized to a single phase tetragonal form at room temperature. Normally, CeO_2 and Y_2O_3 are used to stabilize ZrO_2 to TZP. Secondly, PSZ is generally a kind of composite consisting of a cubic matrix with a dispersion of tetragonal precipitates. The commercial dopants of PSZ are MgO , Y_2O_3 and CaO .

2.1.3 Transformation toughening

Transformation toughening is one of the toughening mechanisms. In zirconia ceramics, this mechanism enhances its fracture toughness and resistance to fracture. The morphology of a material which shows transformation toughening is like that fine tetragonal zirconia grains are dispersed in a cubic matrix. In the cooling step from the processing temperature, tetragonal grains are constrained from the transformation by the surrounding matrix and consequently can be retained in a metastable tetragonal phase. In transformation toughening, the approaching crack front is the catalyst that triggers the transformation, which in turn the zone ahead of the crack tip is in compression, Given that the transformation ($t-m$) occurs in the vicinity of the crack tip, extra energy is required to extend the crack through that compressive layer, which increases both the toughness and the strength of zirconia ceramics. This mechanism is not only working in the TZP and PSZ, but also in the composite of $Al_2O_3-ZrO_2$ and other oxide- ZrO_2 .

2.2 Introduction to Ce-TZP

2.2.1 Literature review of Ce-TZP

The phase diagram of ZrO_2 - CeO_2 was at first reported by P. Duwez and F. Odell (2) in 1950. In 1989, M. Yoshimura (3) reported more exact one similar to Figure 2.1. Figure 2.1 is a phase diagram accepted widely nowadays.

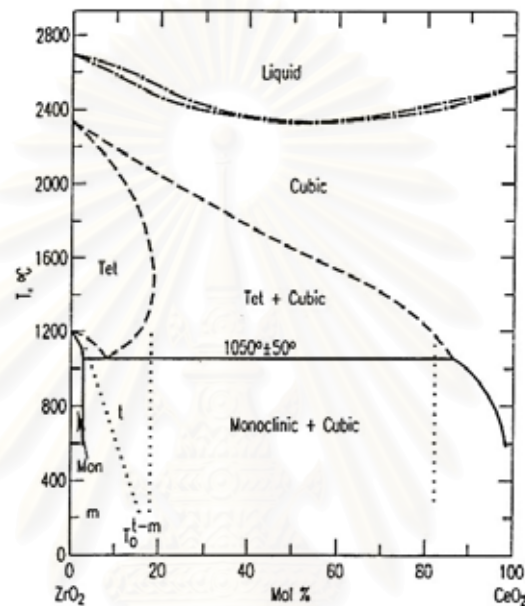


Figure 2.1 Phase diagram of ZrO_2 - CeO_2

In 1986, Koji Tsukuma (4) reported “Mechanical properties and thermal stability of CeO_2 containing tetragonal zirconia polycrystals”. In this study commercial grade of various CeO_2 content-zirconia used as raw powders were sintered at various temperatures. The result of this experiment showed that 12 mol% Ce-TZP exhibited remarkable fracture toughness and high bending strength.

From the phase diagram in Figure 2.1, the phase of the 12 mol% CeO_2 doped ZrO_2 is tetragonal at sintering temperature range of over $1200^\circ C$ and it can remain tetragonal in metastable form at room temperature.

Ce-TZP was resistant to phase transformation during low temperature aging. This property is the attractive factor for replacing Y-TZP with Ce-TZP. Because, Y-TZP has been reported that strength and toughness degrade by low temperature aging below $500^\circ C$, and this undesirable degradation results from the tetragonal to monoclinic phase transformation.

Tsugio Sato and Masahiko Shimada (5,6) reported the phase changes and the microstructure resulting from low-temperature annealing of Y-TZP in water. Tetragonal ZrO_2 transformed to the monoclinic phase in the surface of the sintered body, accompanied by microcracking. The transformation rate in water, which was much greater than that in air, was first order with respect to surface concentration of tetragonal ZrO_2 .

2.2.2 Mechanical properties and applications

The mechanical properties of Ce-TZP are shown in table 2.2.

Table 2.2 Mechanical properties of Ce-TZP

Density (g/cm^3)	6.25
Hardness (GPa)	7-9.5
Fracture toughness ($MPa \cdot m^{-1/2}$)	6-30
Bending strength (MPa)	500-800
Young's modulus (GPa)	215
Thermal expansion co-efficient ($\times 10^{-6} \cdot ^\circ C^{-1}$)	8
Thermal conductivity ($W \cdot m^{-1} \cdot K^{-1}$)	2

Ce-TZP is endowed with a good wear resistant property. Therefore, it can find application as bearings, bushings and cutting-tools. The high fracture toughness and strength make it a good candidate for mechanical devices such as insert part for construction.

2.2.3 Literature review of heat-treatment in reduction atmosphere

Strength of transformation toughened ceramics is improved by introducing residual compressive surface stresses. The methods to produce such compressive layers in transformation toughened ceramics are grinding, impact, chemical destabilization of tetragonal zirconia, low-temperature quenching and etc. (7) Ce-TZP exhibits extraordinary deformation behavior which is reduction-induced effect on its mechanical properties. A special technique to improve the strength of Ce-TZP is heat-treatment in reduction atmosphere. There are two theories that explain the phenomenon of compressive layer surface which occurs after heat-treatment in reduction atmosphere. Firstly, heat-treatment in reduction atmosphere destabilizes the Ce-TZP that make tetragonal (*t*) transform to monoclinic (*m*) phase then volume of surface layer is expanded. The expansion of surface layer generates compression force in the surface of the bulk ceramic. The explanation of this theory is come

from the XRD results that show the destabilization of Ce-TZP after annealing in reduction atmosphere, which is the change of Ce^{4+} to Ce^{3+} . From the phase diagram of $\text{ZrO}_2\text{-}\frac{1}{2}\text{Ce}_2\text{O}_3$ in Figure 2.2., there are monoclinic and tetragonal phase at 12 mol% $\frac{1}{2}\text{Ce}_2\text{O}_3$. Secondly, the reduction atmosphere reduce CeO_2 from Ce^{4+} to Ce^{3+} then the ionic radius of cerium ion changes from 0.094 nm to 0.107 nm.

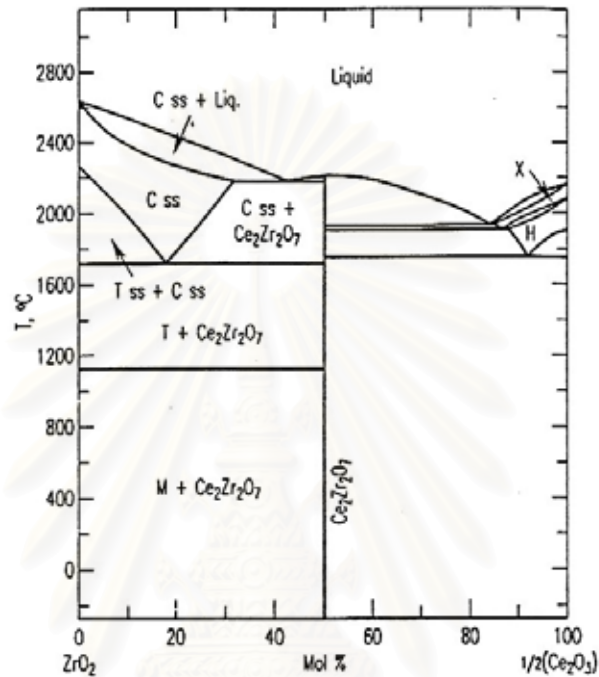


Figure 2.2 Phase diagram of $\text{ZrO}_2 - \frac{1}{2}\text{Ce}_2\text{O}_3$

In 1989, Karl-Heinz and Nils Claussen (8) reported “Strengthening of ceria-doped tetragonal zirconia polycrystals by reduction-induced phase transformation”. They used reduction heat-treatment technique to induce the *t*-to-*m* phase transformation in the surface of Ce-TZP. The annealing condition in the research was 1400 and 1500°C for 2 h in nitrogen atmosphere with MoSi_2 -heated Al_2O_3 tube furnace. The fracture toughness could not be determined by the indentation crack length technique since visible cracks (Figure 2.3) did not initiate at the indent corners.

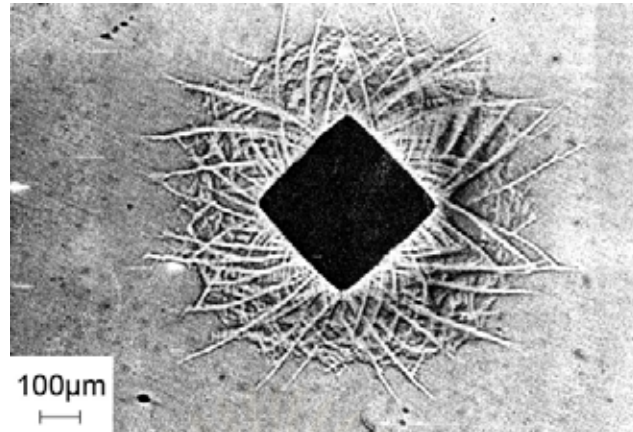


Figure 2.3 The Vickers indentation (load = 1000 N) in hot isostatically pressed 12Ce-TZP

The four-point bending strength of sintered 12 mol% Ce-TZP increased from 240 to 545 MPa after annealing at 1400°C for 2 h in nitrogen. The strength of the same material hot isostatically pressed in oxygen increased from 430 to 595 MPa after it was annealed in nitrogen for 2 h at 1500°C. They explained the destabilization of the *t* phase could be caused by two effects. One was the formation of ZrO₂-CeO_{1.5} solid solution which had no *t* symmetry at ambient temperature (1000°C). The other was the decrease of the CeO₂ content in the ZrO₂-CeO₂ solid solution, and the composition changed to a concentration range of CeO₂ where the *m* phase was stable at low temperature.

C. Zhao et al. (9) reported “High toughness Ce-TZP by sintering in an inert atmosphere”. In this experiment, the specimens were sintered at 1450°C in air and in argon atmosphere by using microwave furnace with SiC susceptor to realize hybrid sintering. The fracture toughness of the specimen which was sintered in argon atmosphere was higher than specimen that sintered in air. Moreover, this experiment reported that the specimen sintered in vacuum using graphite heating element was fully monoclinic, on the other hand the specimen sintered in argon atmosphere showed tetragonal phase with a little monoclinic phase and small amount of cubic phase.

Hideo Hasegawa and Masakuni Ozawa (10) reported “Strengthening mechanism of ceria-doped tetragonal zirconia polycrystals by heat treatment in reducing atmosphere”. The heat treatments of specimens were carried out in the temperature range of 600 to 1000°C for 0-4 h in flowing hydrogen gas. The heat treatments were conducted with a conventional-type electric furnace and occasionally an infrared gold image furnace (RHL-P610CP, Sinku-Riko, Inc.) which was suitable for heating in short time. The specimen reduced at 800°C for 60 s showed the hardening of the material and it continuously increased from the interior

towards the surface. The lattice volume of a fully reduced tetragonal phase of 12Ce-TZP was 0.13900 nm^3 , which was 1% larger than the untreated specimen with 0.13774 nm^3 . The weight loss was due to the released oxygen in a specimen, which was induced by the valence change of Ce^{4+} to Ce^{3+} . The change was described as the following equation.

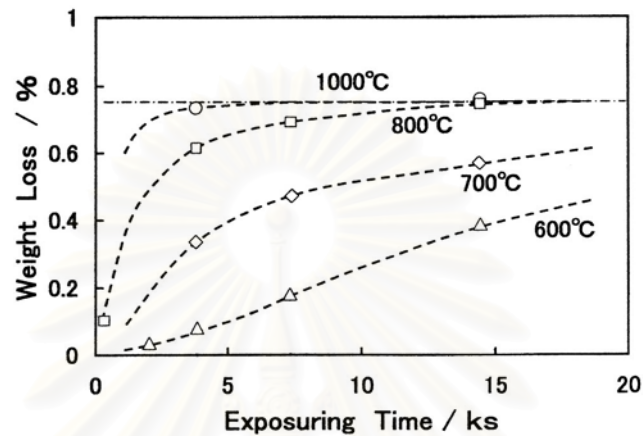
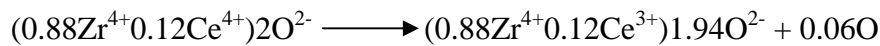


Figure 2.4 Weight loss versus annealing time in reduction heat treatment in flowing hydrogen gas at 600, 700, 800 and 1000°C for 12Ce-TZP

The weight loss of annealed specimen, which is shown in Figure 2.4, is increased by the increasing of soaking time and annealing temperature. The reduction of Ce cation induced the lattice volume expansion of Ce containing phase, and it led to the introduction of the residual compressive stress in the surface and then improved the mechanical properties of ceramic. The reduction-induced strengthening (RIS) mechanism would be widely applied to CeO_2 containing ceramics.

Matsuzawa et al. (11) reported “The effect of reduction on the mechanical properties of CeO_2 doped tetragonal zirconia ceramics”. In this experiment, they compared the change in four types of ZrO_2 material such as 12Ce-TZP, 3Y-TZP, 8Y-FSZ and 9Mg-PSZ. The specimens were heat-treated in a hydrogen atmosphere from room temperature to 1000°C over a period of 1.5 h in an electric furnace. The samples were maintained at this temperature for 8 h, after which, the furnace was cooled and the samples removed from the hot zone to promote rapid cooling. In order to avoid re-oxidation of samples, they were cooled to room temperature with the hydrogen replaced by argon gas. The weight loss during the heat treatment amounted to about 0.74% in Ce-TZP, but was less than 0.1% in the other materials. The fracture toughness decreased from 12.2 to 2.3 $\text{MPa}\cdot\text{m}^{1/2}$. In contrast, the hardness effectively increased from 9.5 to 12.5 GPa after the reduction. After final process of the

re-heating at 1000°C in air, the weight and mechanical properties were all recovered to their original level.

J. Vleugels et al. (12) reported “Toughness enhancement of Ce-TZP by annealing in argon”. The sample were annealed by hybrid microwave heating (Cera Lab II, MEAC, Belgium) in an Ar atmosphere with 5 vol% N₂ at different temperatures between 1200 and 1450°C and different holding time. Optimum mechanical properties were obtained after 10-20 min annealing at 1450°C. The surface toughness of annealed sample increased from 8 to 16 MPa·m^{1/2}, whereas the initial hardness of 10 GPa decreased only 7% due to the larger grain size.

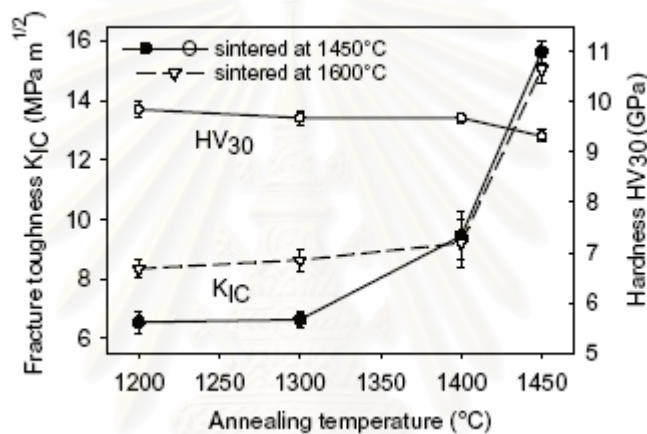


Figure 2.5 Fracture toughness and hardness, obtained from surface indentations, after 20 min annealing in Ar (5% N₂) at different temperatures. The starting samples were sintered in air for 1 h at 1450 or 1600°C

The influence of the annealing temperature at a constant annealing time of 20 min on toughness and hardness on the surface of the sample, is presented in Figure 2.5. When the annealing temperature of the ceramic sintered at 1450°C increased from 1200 to 1450°C, the fracture toughness increased from 6 up to 15.8 MPa·m^{1/2}, whereas the initial hardness of 10 GPa only decreased by 7%.

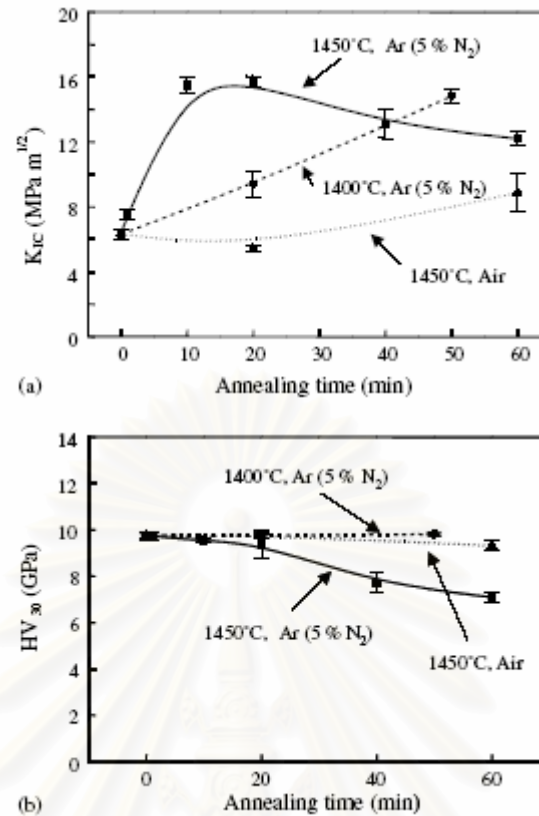


Figure 2.6 Fracture toughness (a) and Vickers hardness (b), obtained from surface indentations, as a function of annealing time and temperature in air and Ar (5% N_2). Starting sample was sintered in air for 60 min at 1450°C

The evolution of the indentation toughness on the outer surface of the sample as a function of annealing time at different temperatures under inert atmosphere and air are shown in Figure 2.6a. When annealed in air at 1450°C, only a slight increase in K_{IC} was noticed after 1h, whereas under inert atmosphere the toughness was found to linearly increase with annealing time at 1400°C. At 1450°C in the inert atmosphere, the toughness initially increased very fast to a maximum of $15.8 \text{ MPa}\cdot\text{m}^{1/2}$ after 10 min, but decreased at longer annealing time. No significant change in hardness was observed for the samples annealed in air at 1450°C or annealed in Ar at 1400°C, as shown in Figure 2.6b.

CHAPTER 3

EXPERIMENTAL PROCEDURE

3.1 Experimental procedure

The experimental procedure including sample preparation and characterization are shown in Figure 3.1 and Figure 3.2, respectively.

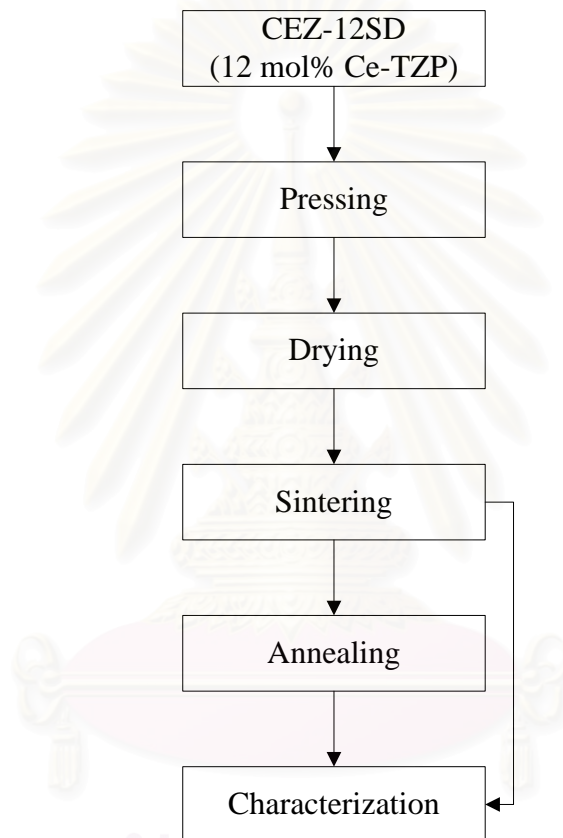


Figure 3.1 Flow chart of experimental procedure

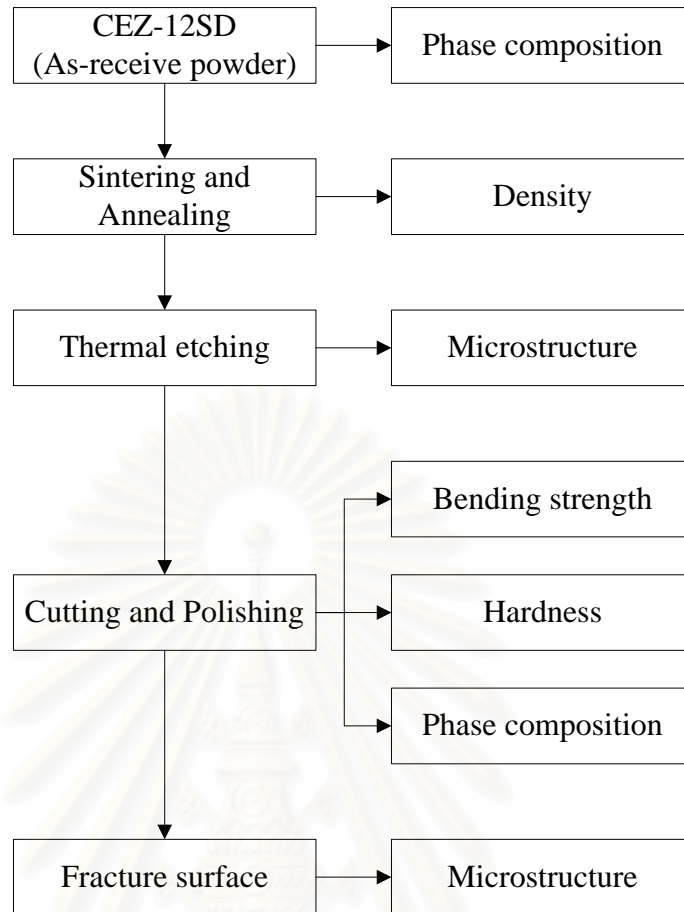


Figure 3.2 Flow chart of characterization

3.2 Raw material

The starting material in this study was commercial grade 12 mol% Ce-TZP powder (CEZ-12SD, Daiichi-Kigenso Kagaku Kogyo Co.,Ltd., Japan). The chemical composition of this powder is shown in Table 3.1.

Table 3.1 The chemical composition and other properties of CEZ-12SD powder

Chemical analysis	
ZrO ₂ +HfO ₂	83.02%
CeO ₂	15.99%
Na ₂ O	0.004%
CaO	0.005%
Al ₂ O ₃	0.25%
H ₂ O	0.26%
Properties	
Loss of ignition	0.07%
Surface area	10.7 m ² /g
Average particle size	0.32 μm

3.3 Sample preparation

Two grams of powder was uniaxially pressed into pellets with a diameter of 20 mm under a pressure of 20 MPa. 55 grams of powder was pressed into square plate using 51x75 mm die under the same pressure to get test specimens for bending strength. The samples were sintered at 1350-1550°C for 2 h with a heating rate and cooling rate of 5°C/min using an electric furnace. Specimens were set on an Al₂O₃ sagger without a cover. The heat-treatment was performed using high temperature furnace (Himulch 5000, Fujidempa K.K.). The specimens sintered at 1450°C and 1550°C were heat-treated at 1100-1200°C for 15-60 min in vacuum atmosphere (2×10^{-2} Pa) with a heating and cooling rate of 10°C/min. The specimen was set in a BN sagger and the sagger was set in a larger carbon container. The remark of annealed specimens is shown in table 3.2.

Table 3.2 The remark of annealed specimens

Annealing temperature (°C)	Annealing time (min)		
	15	30	60
1100	1450HTV1100x15	1450HTV1100x30	1450HTV1100x60
	1550HTV1100x15	1550HTV1100x30	1550HTV1100x60
1200	1450HTV1200x15	1450HTV1200x30	1450HTV1200x60
	1550HTV1200x15	1550HTV1200x30	1550HTV1200x60

3.4 Characterization

3.4.1 Density

The bulk density and water absorption were measured by Archimedes' method (13) according to ASTM C 830-93. The theoretical density calculated from measured X-ray data is 6.26 g/cm³.

3.4.2 Bending strength

The bending strength of the specimens was measured by the 4-point bending method according to JIS-R1601. (14) The sintered specimens were cut into 3x4x40 mm by diamond blade and wheel at BIWAJIMA GIKEN, Japan. The edges of specimen were chamfered by #800 and #1200 mesh silicon carbide papers. The top surface of specimens was polished with silicon carbide powder number #2,000 and #8,000 mesh, respectively on a glass plate and finished with 6, 3 and 1 μm diamond paste. After polishing, the specimens were cleaned with

alcohol and washed in ultrasonic bath to remove dirt and polishing powder from the surface. The polished surface was observed by optical microscope to confirm that it did not have pores and scratch lines. The testing machine was a using universal testing machine (Instron) with a loading speed of 0.5 mm/min at the loading points on the specimens.

The 4-point bending strength is calculated by the following equation:

$$\sigma_{b4} = \frac{3P(L-l)}{2wt^2}$$

Where:	σ_{b4}	=	4-point bending strength (N/mm ²)
	P	=	Maximum load at break of specimen (N)
	L	=	Distance between lower supporting points (mm)
	l	=	Distance between upper loading points (mm)
	w	=	Width of specimen (mm)
	t	=	Thickness of specimen (mm)

3.4.3 Vickers hardness

The hardness and fracture toughness of the specimens were determined by the Vickers indentation method (Instron Wolpert 930/250 in MTEC) and calculated according to JIS-R1610 (15) and JIS-R1607 (16), respectively. Vickers indentation was applied at the load of 98.07, 294.21 and 490.35 N (10, 30 and 50 kg), respectively to the polished surface of specimens with loading time 5 s and soaking time 15 s.

Vickers hardness is calculated by the following equation:

$$H_v = 1.8544 \left(\frac{P}{d^2} \right)$$

Where:	H _v	=	Vickers hardness (Pa)
	P	=	Load (N)
	D	=	Diagonal length (mm)

Fracture toughness is calculated by following equation:

$$K_{IC} = 0.018 \left(\frac{E}{Hv} \right)^{1/2} \left(\frac{P}{C^{3/2}} \right)$$

Where: K_{IC} = Fracture toughness
 E = Young's modulus
 C = Crack length (mm)

3.4.4 Microstructure

The microstructure of specimens was observed by optical microscope (Olympus BX60M) and scanning electron microscope (SEM, JEOL:JSM-1670). The three kinds of surfaces, polished followed by thermal etching, polished followed by annealing and fractured surfaces, were observed. The polished surface was prepared using the same method as the bending strength specimen. The thermal-etching condition was 1400°C for 15 min with a heating rate of 5°C/min. The specimen after bending test was used to observe fractured surface. The purpose of observation of different surfaces is to investigate the grain size, the morphology of the surface after annealing and the origin of cracks, respectively.

3.4.5 Phase analysis

Two kinds of samples, as-received powder and sintered specimens, were observed for the phase composition by x-ray diffraction (XRD, Bruker D8-Advanced). The X-ray diffraction conditions were $2\theta = 20-40^\circ$, x-ray energy 40 kV 40 mA, scanning speed 3°/min and using $CuK\alpha$ radiation.

CHAPTER 4

RESULTS AND DISCUSSION

4.1 Raw material characterization

The chemical composition, average particle size and other properties of as-received powder are reported in Table 3.1.

4.1.1 Phase analysis

The XRD pattern of CEZ-12SD powder is shown in Figure 4.1. The phase composition is mainly composed of tetragonal zirconia which is solid solution of ZrO_2-CeO_2 ($Zr_{0.88}Ce_{0.12}$) and only small amount of monoclinic phase.

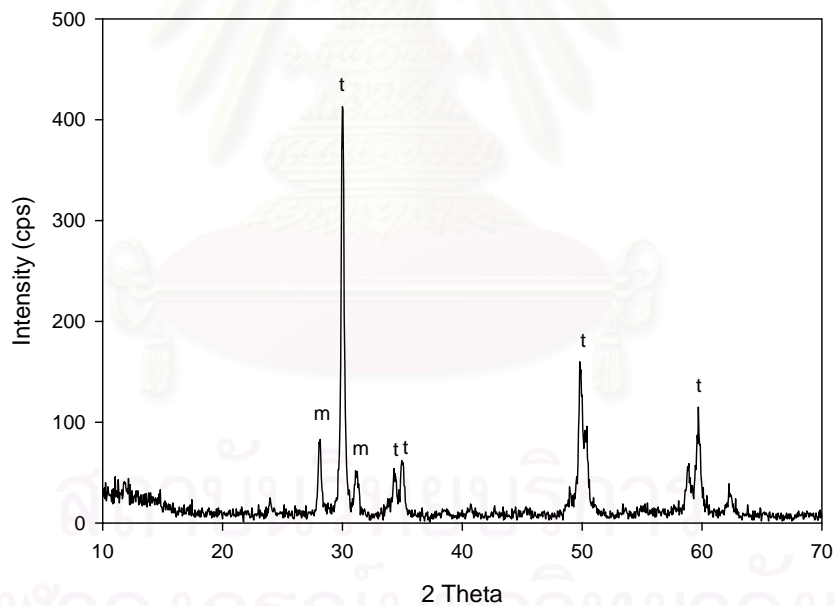


Figure 4.1 XRD pattern of as-received CEZ-12SD.

4.2 Sintered specimen characterizations

4.2.1 Relative density

The specimens were sintered at various temperatures 1350 to 1550°C for 2 h. The relationship between relative density, water absorption and sintering temperature are shown in Figure 4.2. The relative density increases slightly with elevating sintering temperature (1350-1450°C) and it reaches to almost full density when the sintering temperature is higher than 1450°C. The water absorption decreases to zero when the sintering temperature is higher than 1450°C. The density of specimens sintered at 1550°C is 6.23 g/cm³ which is very close to the theoretical density (6.25 g/cm³).

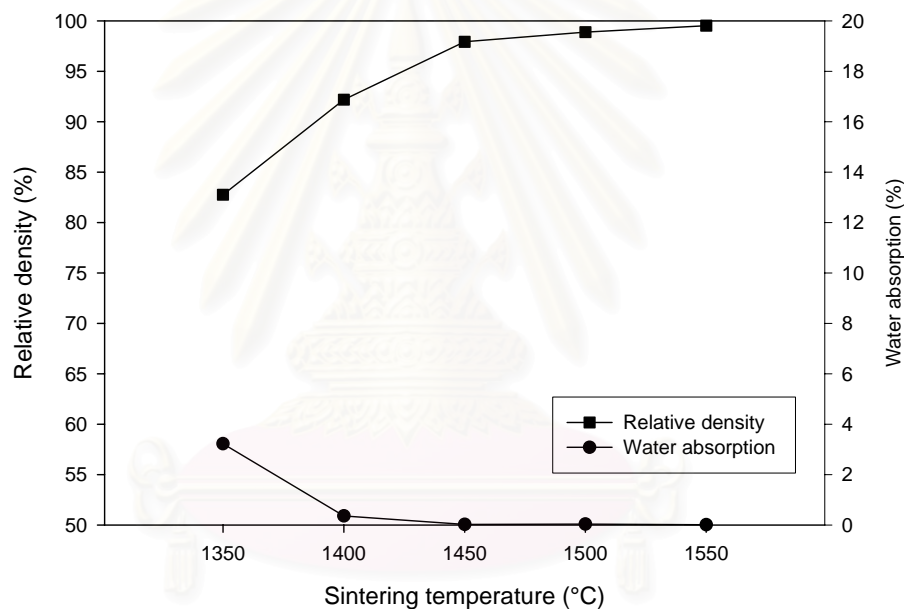


Figure 4.2 Relationship between relative density and sintering temperature.

4.2.2 Average grain size

SEM micrograph of Ce-TZP is shown in Figure 4.3. The average grain size is shown in Figure 4.4. The average grain size increases with increasing the sintering temperature. The micrographs of specimen sintered at 1500 and 1550°C are shown in Appendix 1.

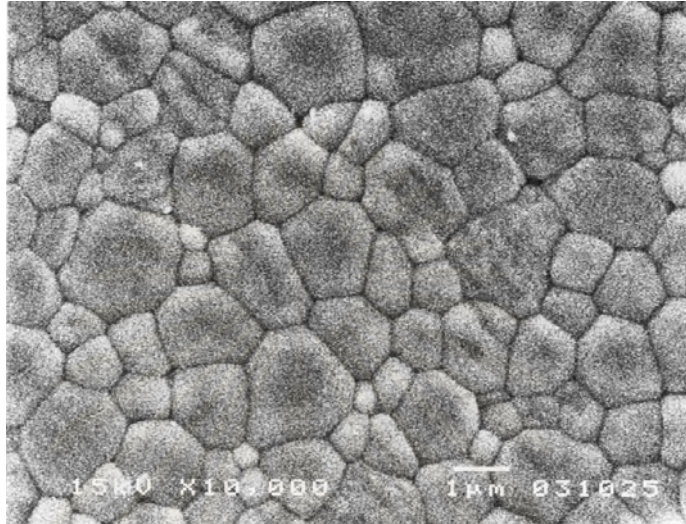


Figure 4.3 SEM micrograph of Ce-TZP sintered at 1450°C and thermal etched.

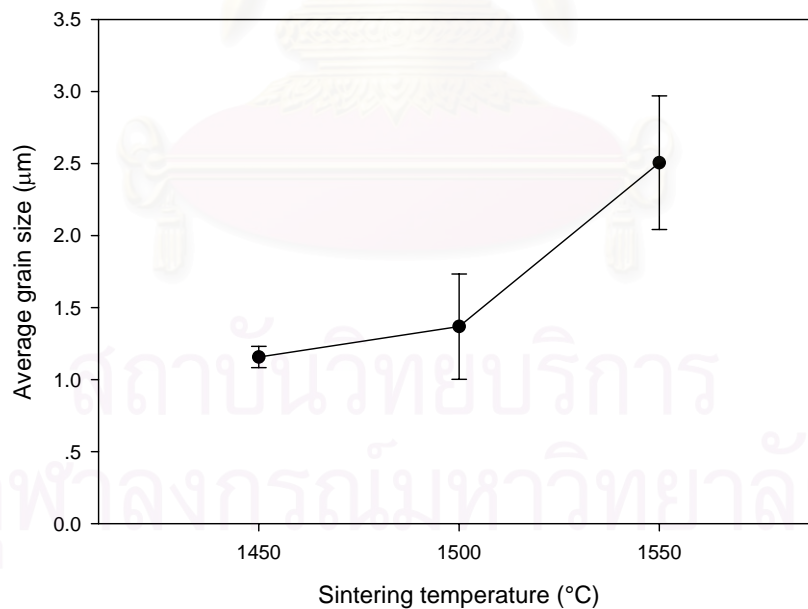


Figure 4.4 Average grain size of Ce-TZP sintered at 1450-1550°C.

4.2.3 Phase analysis

The XRD patterns of specimen sintered at 1450 and 1550°C are shown in Figure 4.5. The crystal phase after sintering is pure tetragonal phase.

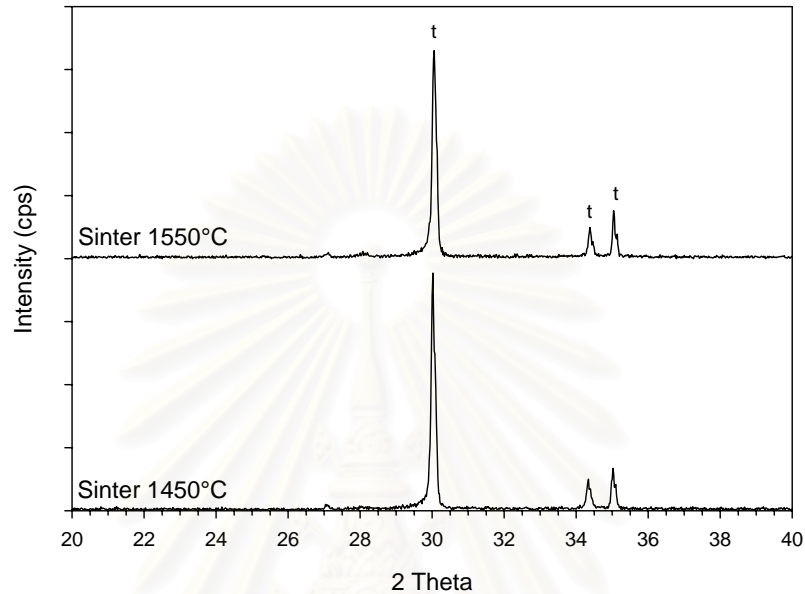


Figure 4.5 X-ray diffraction patterns of the specimens sintered at 1450°C and 1550°C.

4.3 Annealed specimen characterizations

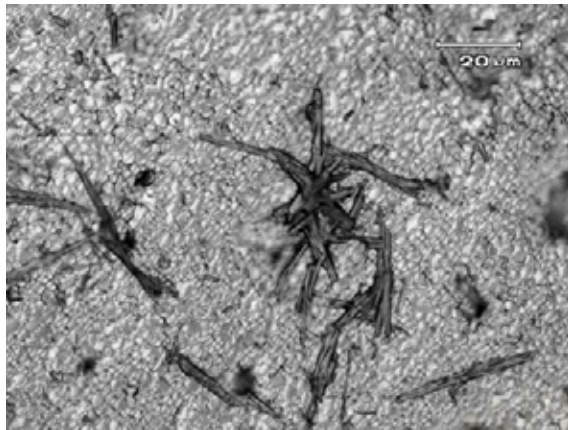
4.3.1 Preliminary annealing of pellet

The pellet specimens sintered at 1450-1550°C were preliminary annealed at 1100-1400°C with a soaking time of 30 min in vacuum to decide the annealing temperature for bar specimens. The color of specimen is shown in Figure 4.6. The color of the sintered specimens is yellowish white. After annealing at 1100-1300°C, the color is changed from dark cream to dark brown. The color of top surface of specimens that annealed at 1400°C changes to gray and the inside color changes to black. At the annealing temperature of 1300°C, the top surface of specimen has only color change but there are abnormal grains and some cracks on the bottom side, which is shown in Figure 4.7 (a). The specimens annealed at 1400°C have large macrocracks at the edge of specimen and the surface of specimen becomes rough, which is shown in Figure 4.7 (b) and Figure 4.7 (c). We conclude that these defects occur from the excess of reduction that increases with elevating of the annealing temperature. From this

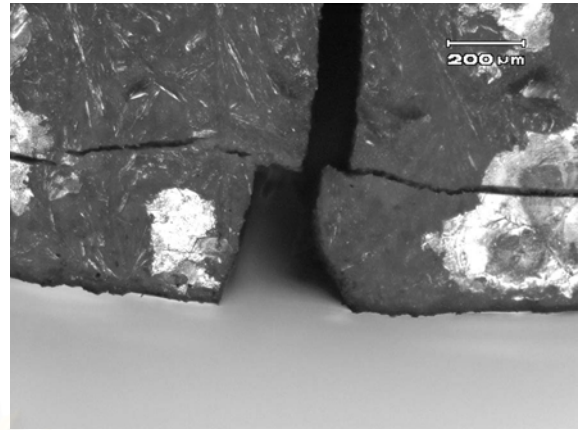
result, the annealing temperature range of 1300-1400°C was omitted in the following experiment. XRD data of these specimens are shown in Appendix 2.



Figure 4.6 Colors of specimen sintered at 1450-1550°C and annealed at 1100-1400°C with a soaking time of 30 min, top side (left) and bottom side (right)



(a)



(b)



(c)

Figure 4.7 Optical micrographs of Ce-TZP sintered at 1550°C, annealed at 1300°C (a) bottom surface annealed at 1400°C (b) edge of top surface and (c) bottom surface

สถาบันวิทยบริการ
จุฬาลงกรณ์มหาวิทยาลัย

4.3.2 Weight loss of annealed specimens

The relationship between weight loss and annealing time of specimens which were annealed at 1100 and 1200°C in vacuum is shown in Figure 4.8 and data of weight loss are shown in Appendix 3. From the result, weight loss increased with increasing annealing temperature. At the soaking time of 15 and 30 min, the weight loss is quite different. But after the longer soaking time to 60 min, the weight loss is the same as that of 30 min. This weight loss after annealing in vacuum is explained by the oxygen vacancy induced from the reduction of CeO_2 to Ce_2O_3 . Weight loss after annealing is too small when compare with the previous researches (10,11) that showed the maximum weight loss was 0.74 wt%. The previous researches were performed in hydrogen atmosphere. The difference between the weight loss of less than 0.02 wt% in our experiment and 0.74 wt% can be explained by the difference of atmosphere that the reduction of CeO_2 to Ce_2O_3 occurs in hydrogen atmosphere but practically, reduction does not occur in vacuum.

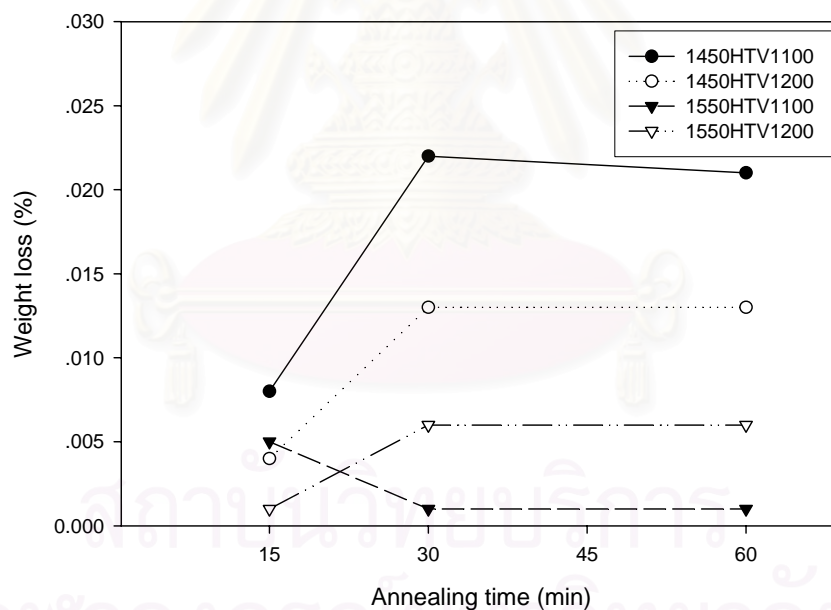


Figure 4.8 Relationship between weight loss and annealing time of specimens annealed at 1100 and 1200°C

4.3.3 Color of annealed specimens

The colors of annealed specimen are shown in Figure 4.9. The color of sintered specimen at 1450°C is yellowish white and light gray for specimens sintered at 1550°C. After annealing, the color of specimen sintered at 1450°C changes to light brown and that of 1550°C to dark brown. The color is darker with increasing annealing time.

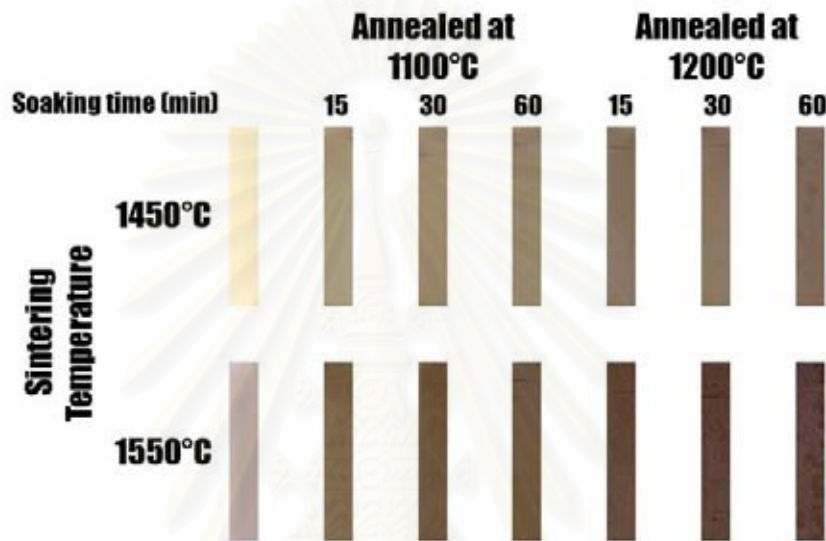
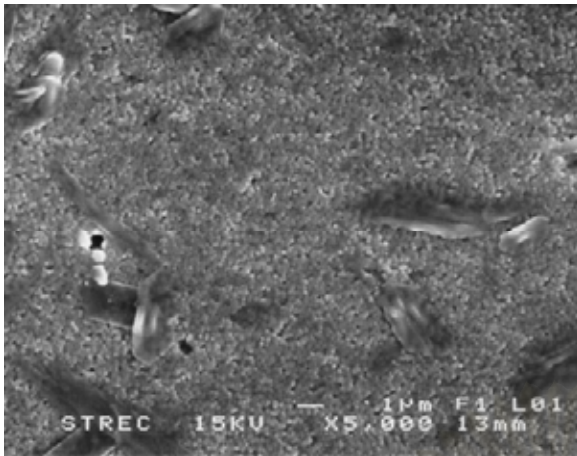


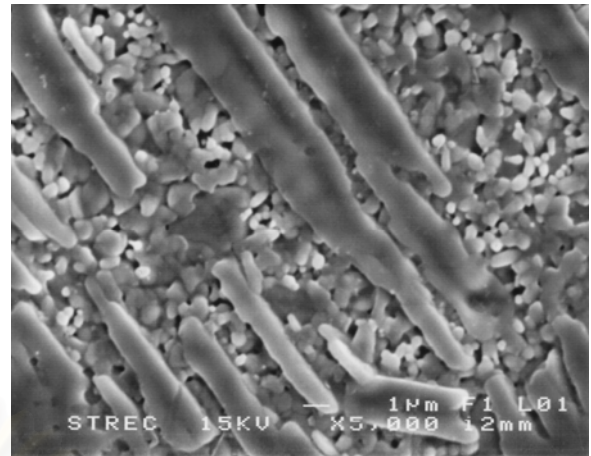
Figure 4.9 Colors of specimen sintered at 1450 and 1550°C and annealed at 1100 and 1200°C with soaking time of 15, 30 and 60 min

4.3.4 Surface observation of annealed specimens

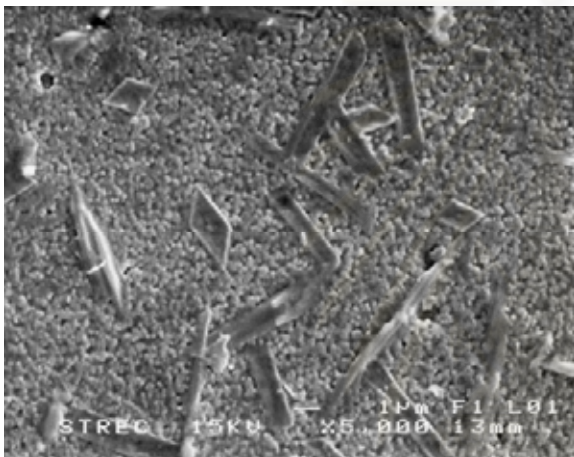
The surface of annealed specimens was observed by SEM. Abnormal grains are observed on the surface. The shape and amount of them are controlled by two factors, annealing temperature and annealing time. Figure 4.10 shows the SEM micrographs of specimens sintered at 1500°C and annealed at 1100-1200°C with soaking time ranging from 15 to 60 min.



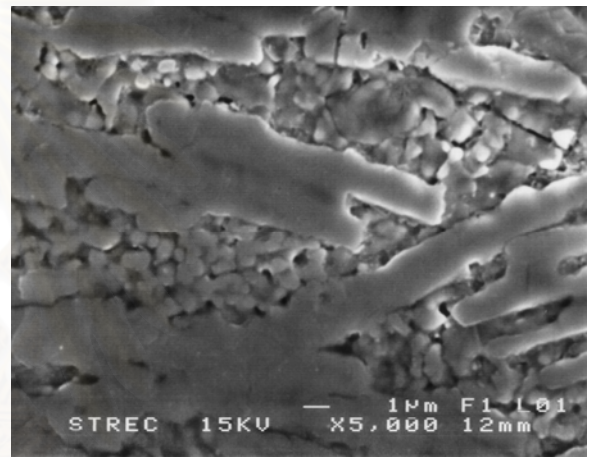
(a)



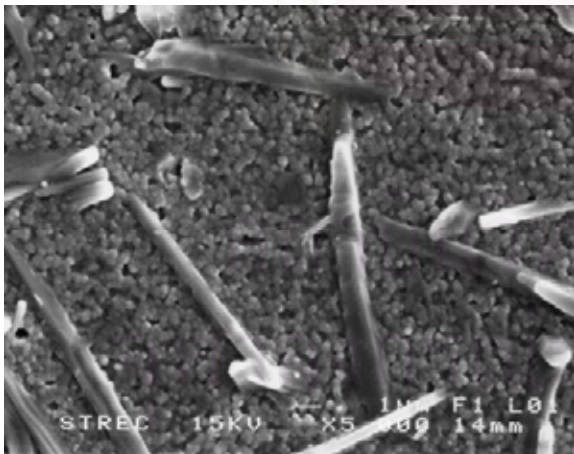
(d)



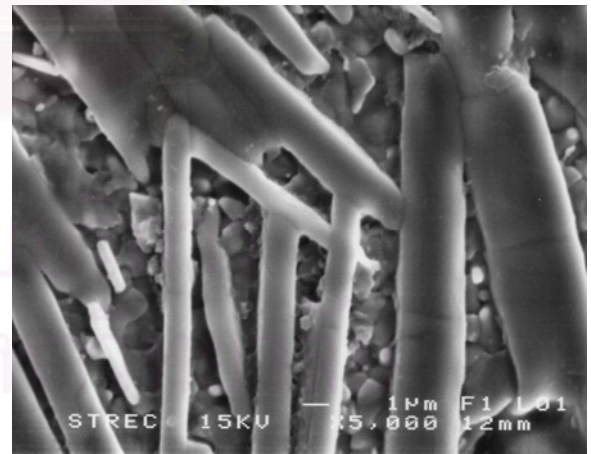
(b)



(e)



(c)



(f)

Figure 4.10 SEM micrographs of specimen sintered at 1550°C and annealed in vacuum at 1100°C and soaking time (a) 15, (b) 30 and (c) 60 min and 1200°C and soaking time (d) 15, (e) 30 and (f) 60 min

Two kinds of grain are observed on the surface. One is the fine grain that distributes on the entire surface and the large grains in needle shape are observed on top of the fine grains. The large grains grow to larger size and increase in amount with increasing temperature and longer soaking time. Both parts were analyzed by EDX are shown in Figure 4.11.

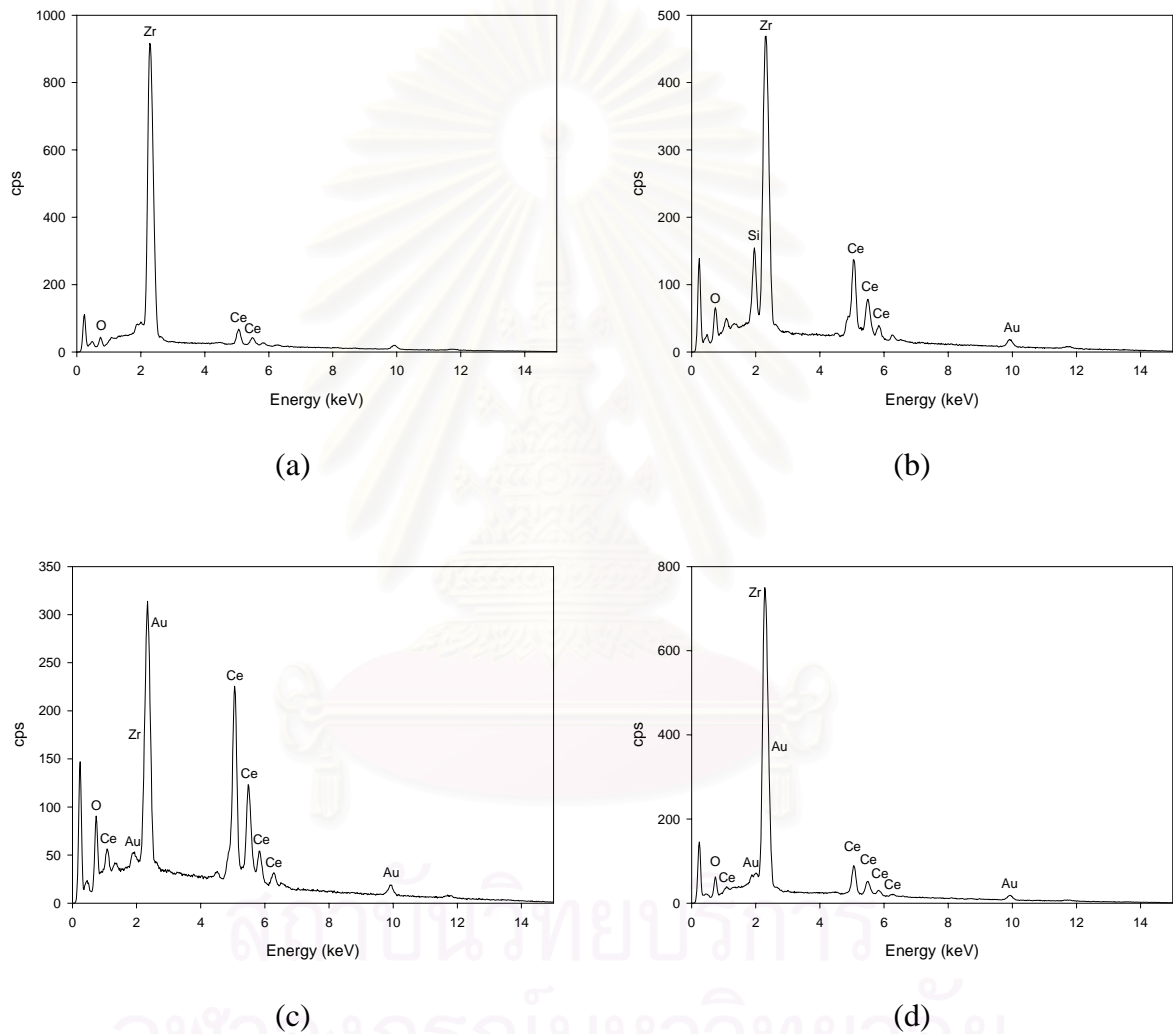
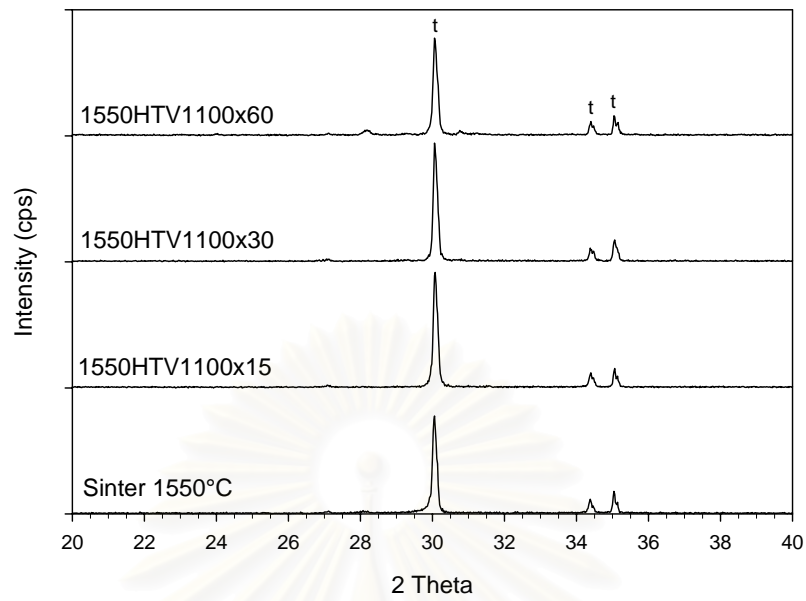


Figure 4.11 EDX patterns of specimen sintered at 1550°C (a), large grain of specimen annealed specimen at 1100°C for 60 min (b), large grain (c) and small grain (d) specimen annealed at 1200°C for 60 min.

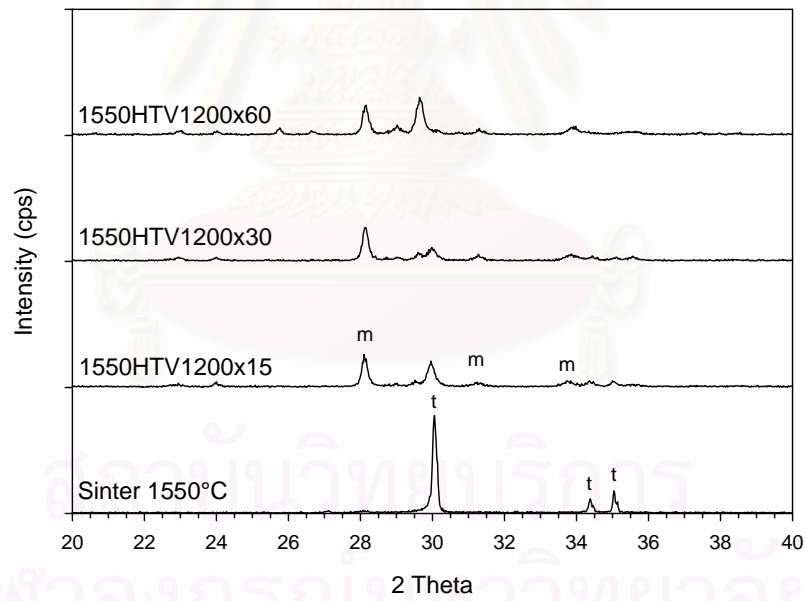
As seen in (a), the peak of Ce is very small in the surface of sintered specimen. Higher Ce peak is observed in the needle like grain in (b). Also higher ratio of Ce peak is observed in (c). Therefore, the needle like grain is regarded as CeO_2 or Ce_2O_3 . It is assumed that the CeO_2 vaporized from the surface during annealing process, and condenses on the surface again. The EDX peak of the fine grain part under the large grain (d) is similar to (a). Therefore, these fine grains might be ZrO_2 . However, the grain size of the fine particles is too small as less than $1\ \mu\text{m}$. On the other hand, the average grain size of Ce-TZP is $1.1\text{-}2.5\ \mu\text{m}$ as shown in Figure 4.3. Crystals observed in the surface is only ZrO_2 as shown in Figure 4.12. Considering all these facts, the fine particles should be ZrO_2 . However, the reason why its grain size is smaller than that of the sintered one cannot be explained. In Figure 4.10, the morphology of large grain shows needle like. However, there are no CeO_2 and Ce_2O_3 peaks. On this point, we have to analyze in more detail in the near future.

4.3.5 Phase analysis of annealed specimens

The XRD patterns of annealed specimen are shown in Figure 4.12. These specimens were annealed at 1100 and 1200°C with 15, 30 and 60 min of soaking time in vacuum. In Figure 4.12 (a), the specimens that annealed at 1100°C in vacuum show the tetragonal phase in all conditions of soaking time. But in Figure 4.12 (b), the tetragonal phase of the specimens that annealed at 1200°C in vacuum decreases and the monoclinic phase increases. The increase of monoclinic phase is thought to come from the destabilization process of Ce-TZP after annealing. The CeO_2 that stabilizes the zirconia vaporizes from the surface of specimen and condenses back on to the ZrO_2 surface during annealing process as seen in Figure 4.10 and Figure 4.11. Then the content of CeO_2 becomes insufficient to stabilize zirconia in the surface. These the monoclinic phase increased with increasing soaking time. And it is thought that the destabilization effect is not sufficient in the annealing at 1100°C .



(a)



(b)

Figure 4.12 XRD patterns of specimens sintered at 1550°C and annealed in vacuum at (a) 1100°C and (b) 1200°C at various soaking time

4.4 Mechanical properties

4.4.1 Hardness (H_v)

The Vickers hardness (H_v) of sintered and annealed specimens are shown in Figure 4.13. In all indentation loadings, no crack occurred from the indent corners. Then the fracture toughness can not be determined by the indentation crack length technique. The optical micrographs of the indented specimens sintered and annealed are shown in Figure 4.14, respectively. The H_v value measured using different loads result in almost the same value as shown in Appendix 4. The H_v of specimens sintered at 1450°C is about 8.0-8.5 GPa. On the other hand, the H_v at 1550°C is in the range of 8.7-9.0 GPa. As seen in Figure 4.2, the relative density of specimens sintered at 1550°C is a little higher than that at 1450°C. The difference of H_v between 1450 and 1550°C may be caused by the density difference. By annealing, the H_v dose not change significantly.



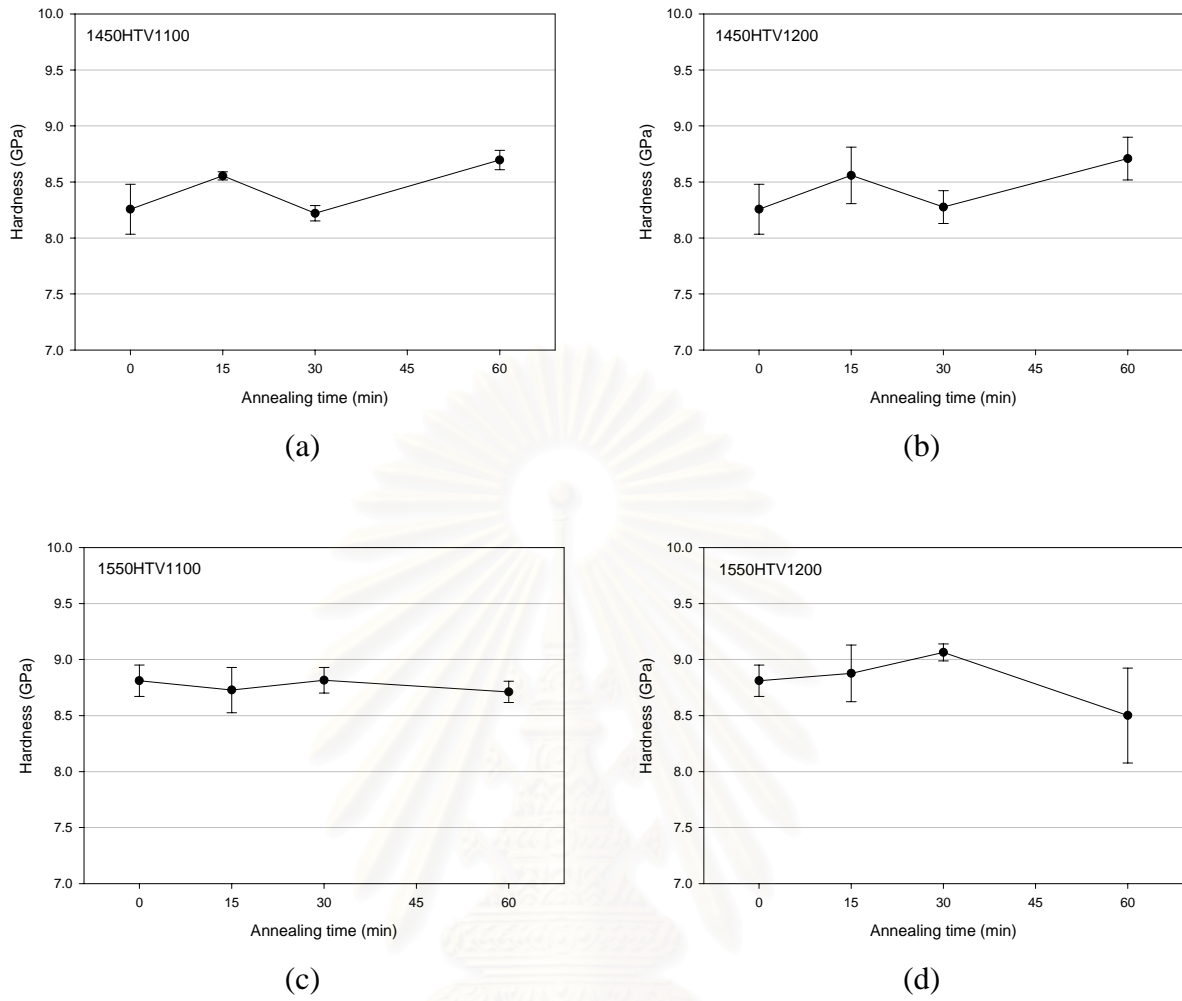


Figure 4.13 Vickers hardness of specimens sintered at 1450 and 1550°C, annealed at 1100 and 1200°C using various soaking time

สถาบันวิทยบริการ
จุฬาลงกรณ์มหาวิทยาลัย

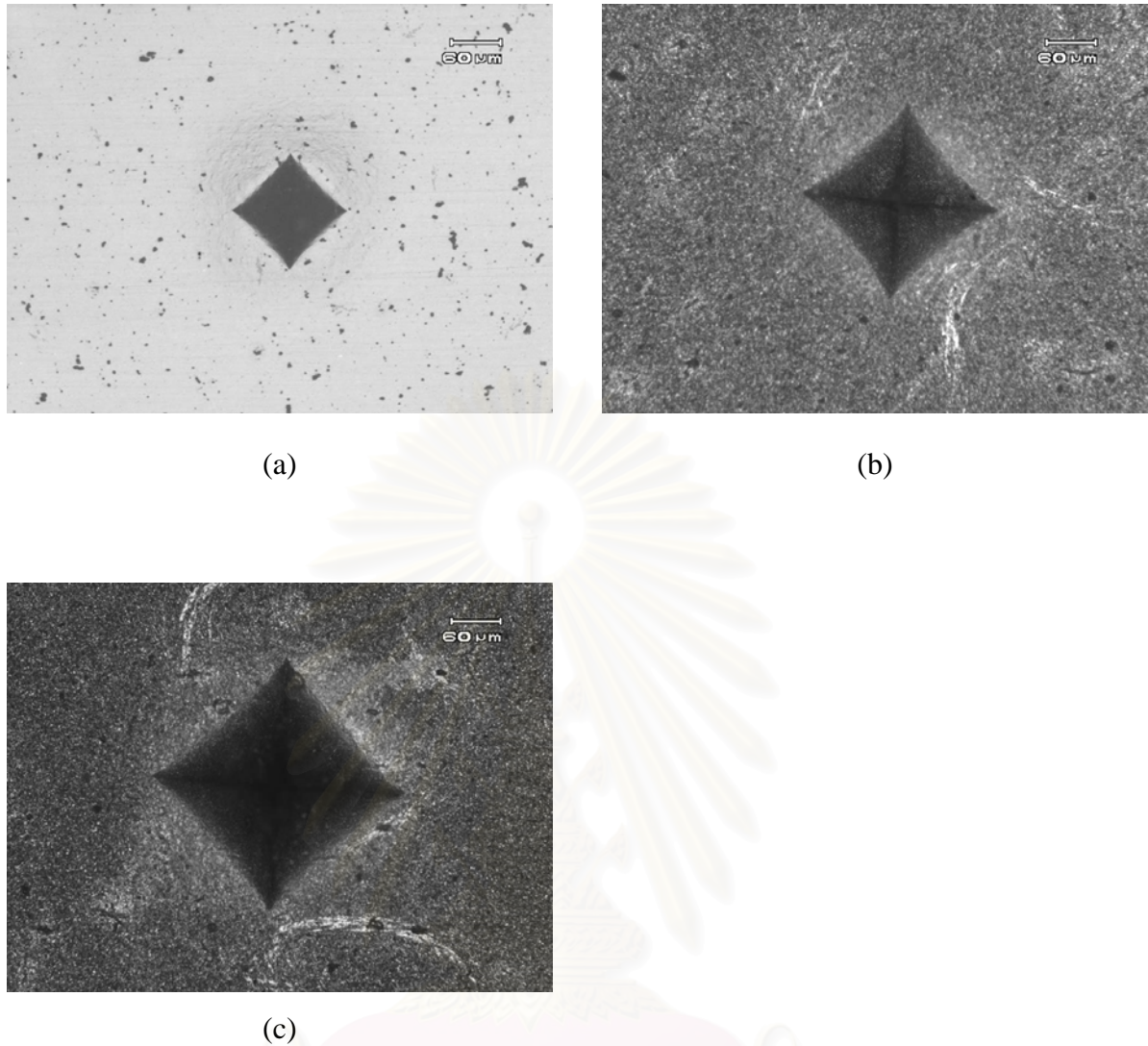


Figure 4.14 Optical micrographs of Ce-TZP sintered at 1550°C with indentation load of 10 kg (a) and annealed at 1200°C, soaking time 15 min with indentation loading of 30 kg (b), 50 kg (c)

4.4.2 Bending strength

The bending strengths of sintered and annealed specimens are shown in Figure 4.15. Bending strength of specimen sintered at 1550°C (555 MPa) is higher than that of 1450°C (480 MPa). This difference of bending strength comes from the bulk density of specimens sintered at 1550°C is higher than that sintered at 1450°C. Annealing at 1100°C, the specimens sintered at both temperatures do not show the change of bending strength. On the other hand, the specimens annealed at 1200°C show the trend of rising strength by increasing soaking time. The change of t - m , which is observed by the XRD (Figure 4.12 (b)), induces volume expansion then we conclude that the increase of bending strength comes from the compressive

layer on the surface of specimen. But in the case of annealing at 1100°C, the phase does not change from the sintered one and the weight loss is too low. Then, the compressive layer does not occur.

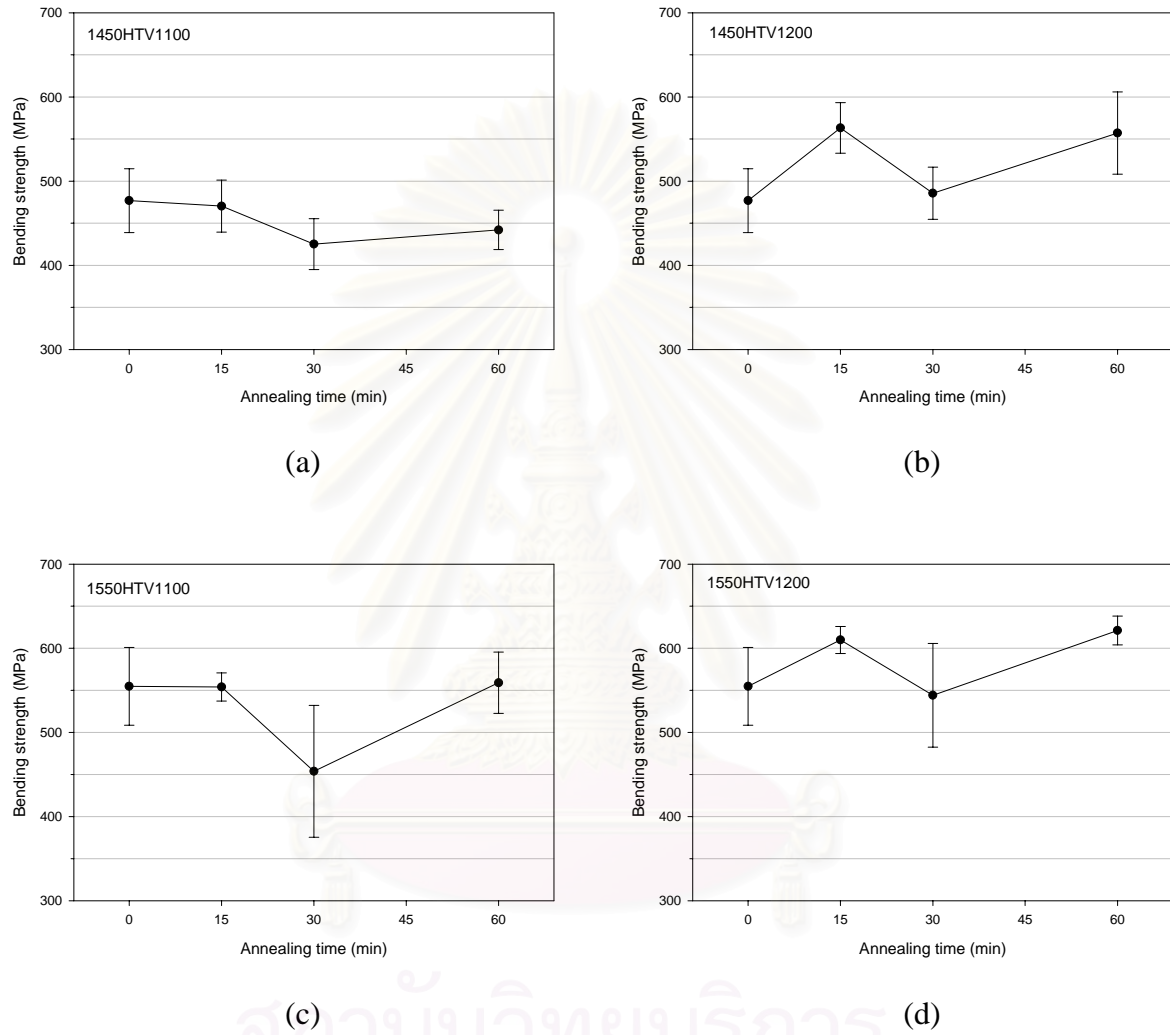


Figure 4.15 Bending strengths of specimens sintered at 1450 and 1550°C, annealed at 1100 and 1200°C with various soaking time

4.5 Comparison between former papers

In the research of Ce-TZP, many researchers used the experiment at the different annealing conditions to develop high mechanical property of Ce-TZP. The difference of annealing atmosphere resulted in the difference of the reduction rate. All of the former researchers used high heating and cooling rate. But in this research we cannot use high cooling rate because of the limitation of the furnace.

Table 4.1 Conditions of annealing and properties after annealing of the former researches and this research

	Annealing atmosphere	Annealing temperature (°C)	Weight loss (wt%)	Crystal phase	Mechanical properties	
					Hardness (GPa)	Strength (MPa)
K.H. Heussner J.Am.Ceram.Soc. 72 [6] 1044-46 (1989)	Ar	1400 and 1500°C for 2 h	n/a	<i>t</i> -ZrO ₂ <i>m</i> -ZrO ₂	n/a	560 (1400°C) 595 (1500°C)
C. Zhap et.al. Scripta Materialia 43 1015-20 (2000)		(Sinter) 1450°C for 20 min	n/a	<i>t</i> -ZrO ₂ <i>c</i> -ZrO ₂ <i>m</i> -ZrO ₂	8.6	n/a
J. Vleugels et.al. Scripta Materialia 50 679-83 (2004)		1200 and 1450°C	n/a	<i>t</i> -ZrO ₂ <i>m</i> -ZrO ₂ (Zr,Ce)O ₂	10	n/a
H. Hasegawa et.al. J.Ceram.Soc.Jp. 111 [4] 252-6 (2003)	H ₂	600-1000°C for 0-4 h rapid cool	0.76%	<i>t</i>	12.8	750
M. Matsuzawa et.al. Acta Materialia 52 1675-82 (2004)		1000°C for 8 h rapid cool	0.74%	<i>t</i>	12.5	n/a
This research	Vacuum	1100- 1400°C	< 0.02	<i>t</i> (at 1100°C) <i>m</i> (at 1200°C)	9.06	621

CHAPTER 5

CONCLUSION

1. 12 mol% Ce-TZP was sintered to full density at 1450-1550°C. Sintered specimens showed pure tetragonal phase. But after annealing, the color of specimen changed from yellowish white to dark brown. The phase of surface annealed at 1100°C was still tetragonal. But after being annealed at 1200°C, the phase changed to pure monoclinic. The weight loss after annealing was less than 0.02%.
2. During annealing, ceria vaporized and condensed back to the surface of specimen. Then, the surface of specimen after annealing had abnormal grains which covered overall the surface. The vaporization might affect the *t-m* destabilization of Ce-TZP.
3. Hardness after annealing didn't change so much. Bending strength after annealing at 1100°C was almost the same with that before annealing. But after annealing at 1200°C, the bending strength slightly increased with increasing annealing time.

CHAPTER 6

FUTURE WORK

The following suggestions are given:

1. The heating rate of annealing should be increase from 10°C/min to 20°C/min to prevent the grain growth.
2. Increase the range of annealing temperature and annealing time to increase data detail.



สถาบันวิทยบริการ
จุฬาลงกรณ์มหาวิทยาลัย

REFERENCES

1. N. Claussen. Mater. Sci. Eng. 71 (1985): 23.
2. P. Duwez and F. Odell. J. Am. Ceram. Soc. 33, 9 (1950): 274-83.
3. M. Yoshimura. Kidorui. 14 (1989): 45-47.
4. Tsukuma, K. "Mechanical properties and thermal stability of CeO₂ containing tetragonal zirconia polycrystals," Am. Ceram. Soc. Bull. 65, 10 (1986): 1386-89.
5. Sato, T. and Shimada, M. "Crystalline phase change in yttria-partially-stabilized zirconia by low-temperature annealing," J. Am. Ceram. Soc. 67, 10 (1984): C212-13.
6. Sato, T. and Shimada, M. "Transformation of yttria-doped tetragonal ZrO₂ polycrystals by annealing in water," J. Am. Ceram. Soc. 68, 6 (1985): 356-59.
7. Green, D.J. "A technique for introducing surface compression into zirconia ceramics," J. Am. Ceram. Soc. 66, 10 (1983): C178-79.
8. Heinz, K. and Claussen, N. "Strengthening of ceria-doped tetragonal zirconia polycrystals by reduction-induced phase transformation," J. Am. Ceram. Soc. 72, 6 (1989): 1044-46.
9. Zhao, C., Vleugels, J., Basu, B. and Van Der Biest, O. "High toughness Ce-TZP by sintering in an inert atmosphere," Scripta mater. 43 (2000): 1015-20.
10. Hasegawa, H. and Ozawa, M. "Strengthening mechanism of ceria-doped tetragonal zirconia polycrystals by heat treatment in reducing atmosphere," J. Ceram. Soc. JP. 111, 4 (2003): 256-56.
11. Matsuzawa, M., Abe, M., Horibe, S. and Sakai, J. "The effect of reduction on the mechanical properties of CeO₂ doped tetragonal zirconia ceramics," Acta Materialia. 52 (2004): 1675-82.
12. Vleugels, J., Zhao, C. and Van Der Biest, O. "Toughness enhancement of Ce-TZP by annealing in argon," Scripta Materialia. 50 (2004): 679-83.
13. ASTM C 830-93 (Reapproved 1998) "Standard test method for apparent porosity, liquid absorption, apparent specific gravity, and bulk density of refractory shapes by vacuum pressure," American Society for Testing and Material (ASTM). New York: ASTM, 1998.
14. JIS R 1601 "Testing method for flexural strength (modulus of rupture) of high performance ceramic," Japanese Industrial Standards (JIS). 1981.

15. JIS R 1610 “Testing method for Vickers hardness of high performance ceramic,” Japanese Industrials Standards (JIS). 1991.
16. JIS R 1607 “Testing method for toughness of high performance ceramic,” Japanese Industrials Standards (JIS). 1995.



สถาบันวิทยบริการ
จุฬาลงกรณ์มหาวิทยาลัย

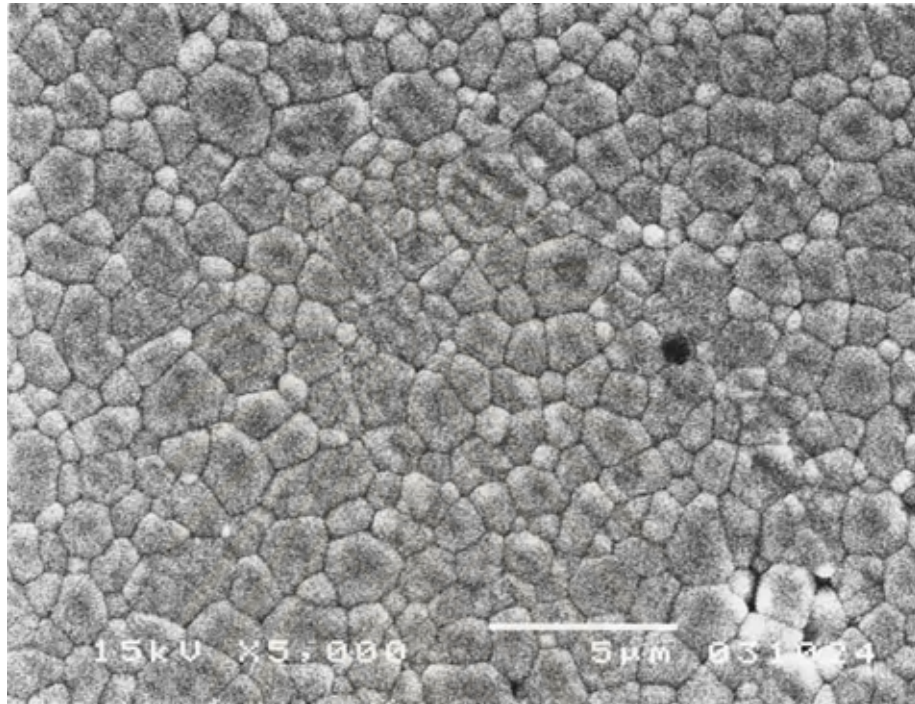


APPENDICES

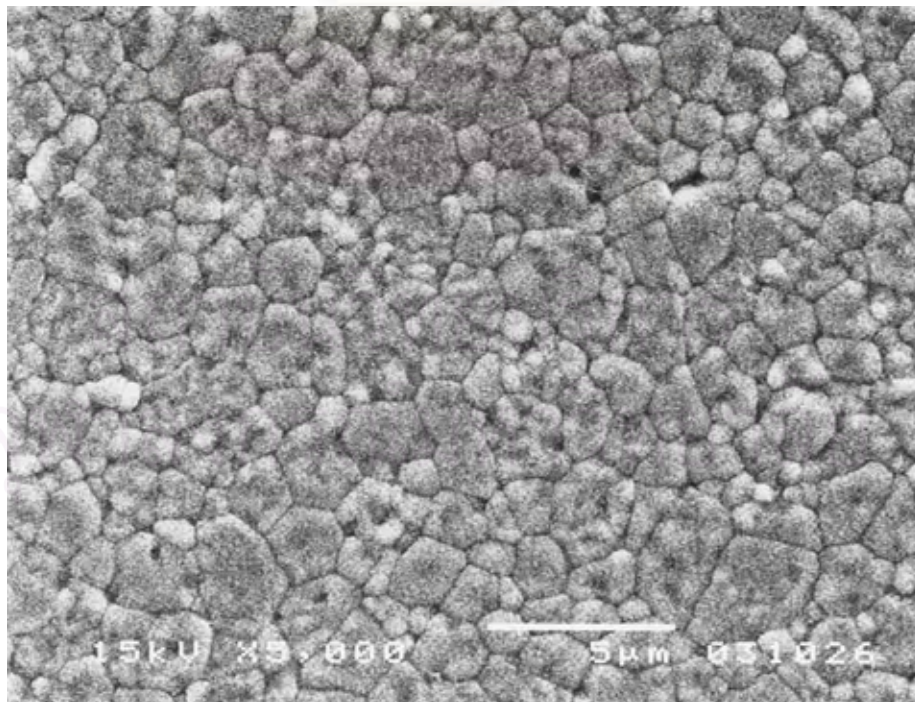
สถาบันวิทยบริการ
จุฬาลงกรณ์มหาวิทยาลัย

Appendix 1

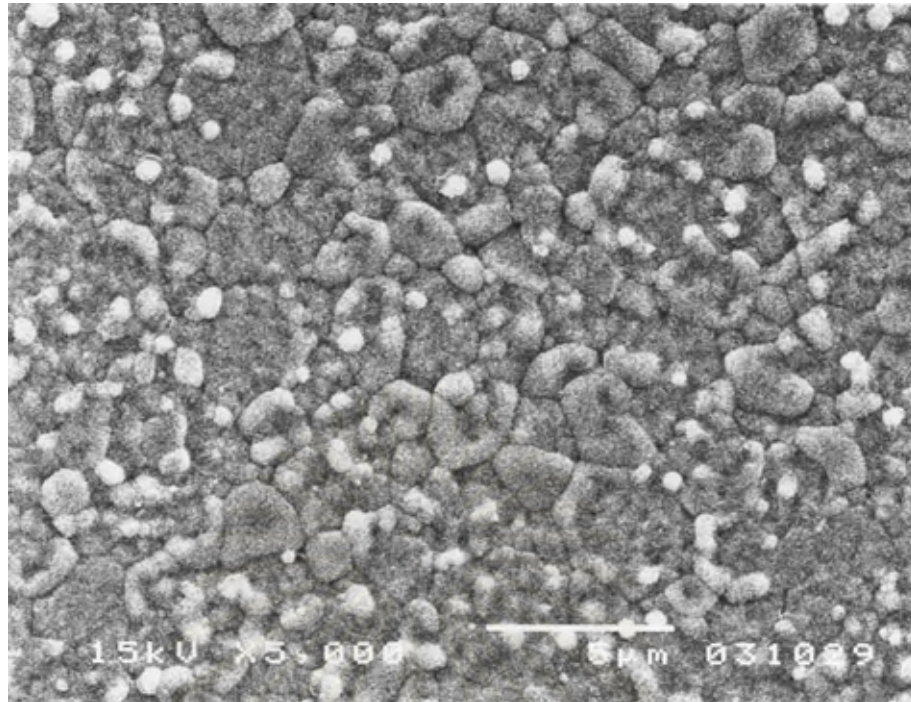
SEM micrographs of specimens sintered at 1450-1550°C and thermal etched at 1400°C for 15 min (a-c), chemical etched in HF (60%) for 5 min (d)



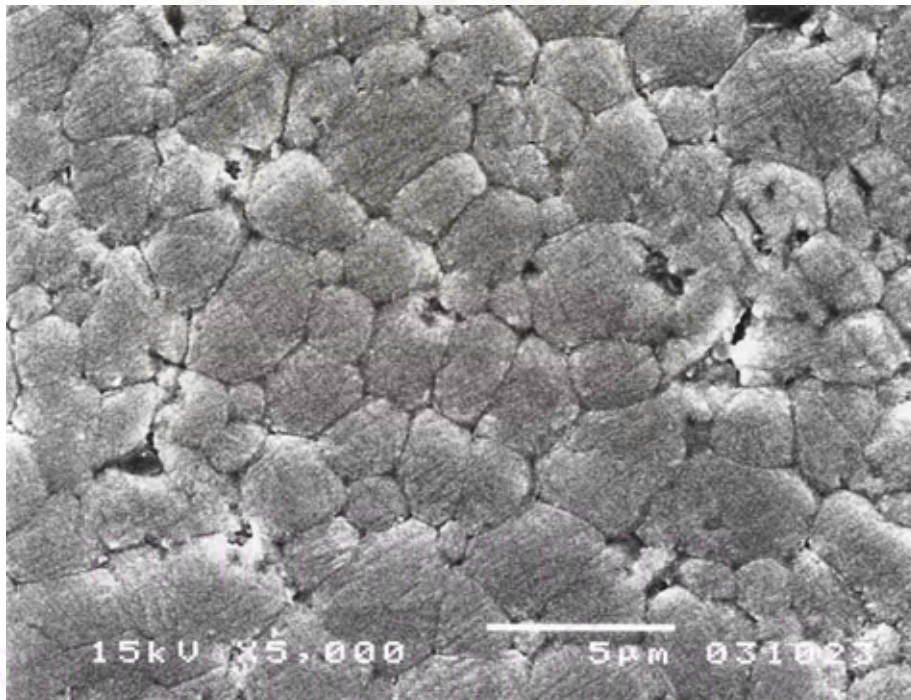
(a) Specimen sintered at 1450°C and thermal etched



(b) Specimen sintered at 1500°C and thermal etched



(c) Specimen sintered at 1550°C and thermal etched

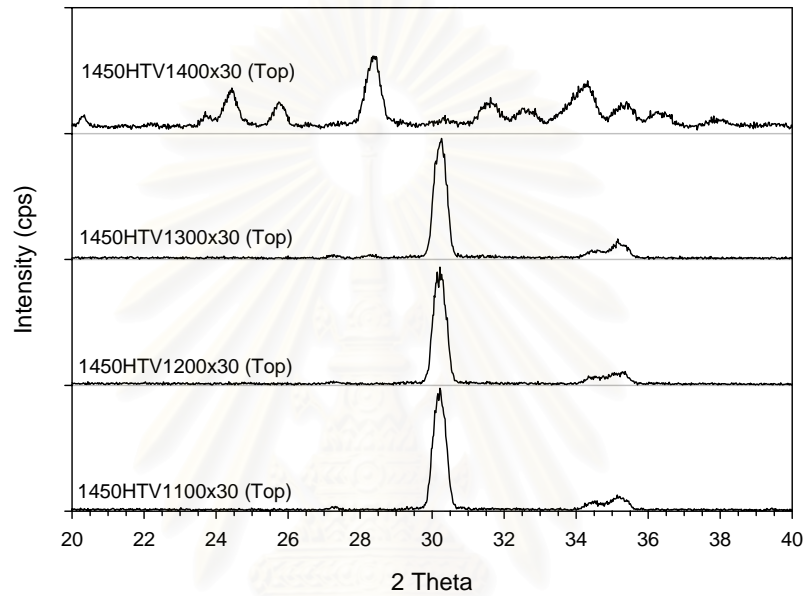


(d) Specimen sintered at 1550°C and chemical etched

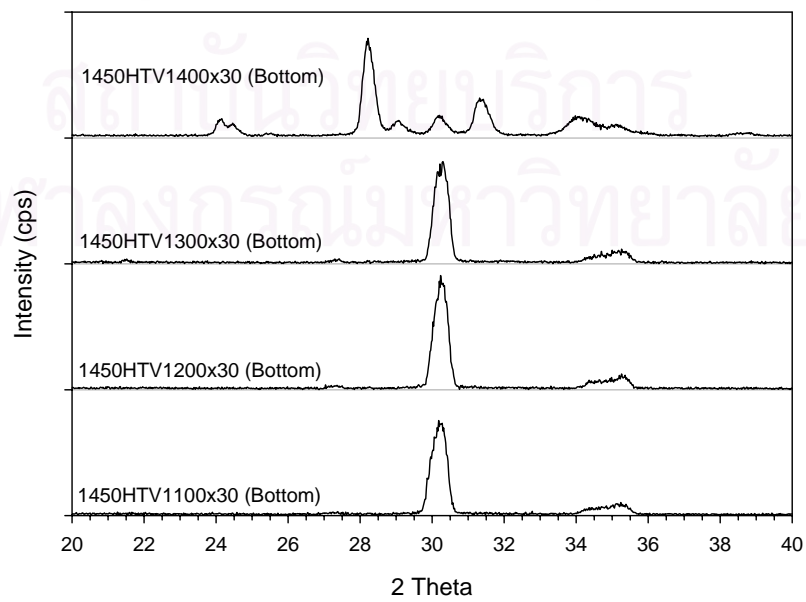
Appendix 2

XRD patterns of preliminary annealed specimens at 1100-1400°C in vacuum

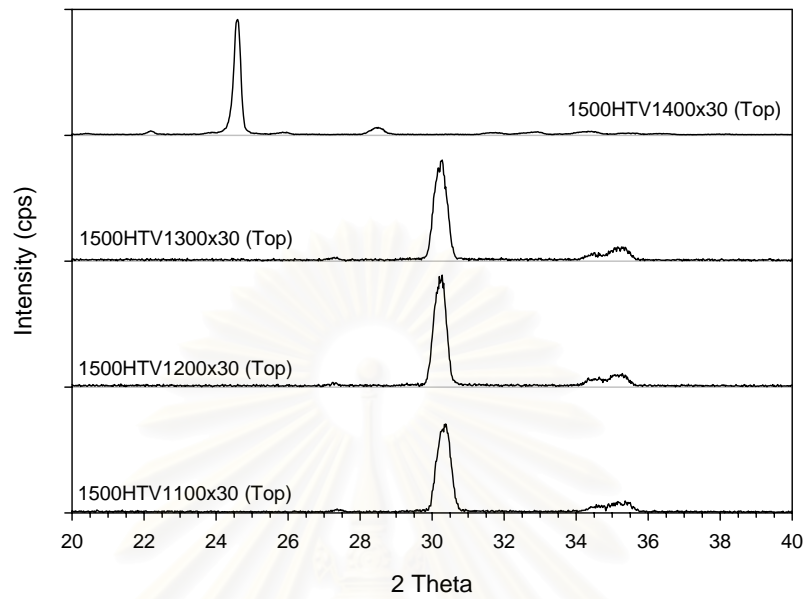
Specimen sintered at 1450°C and
annealed at 1100-1400°C for 30 min in vacuum
(Top surface)



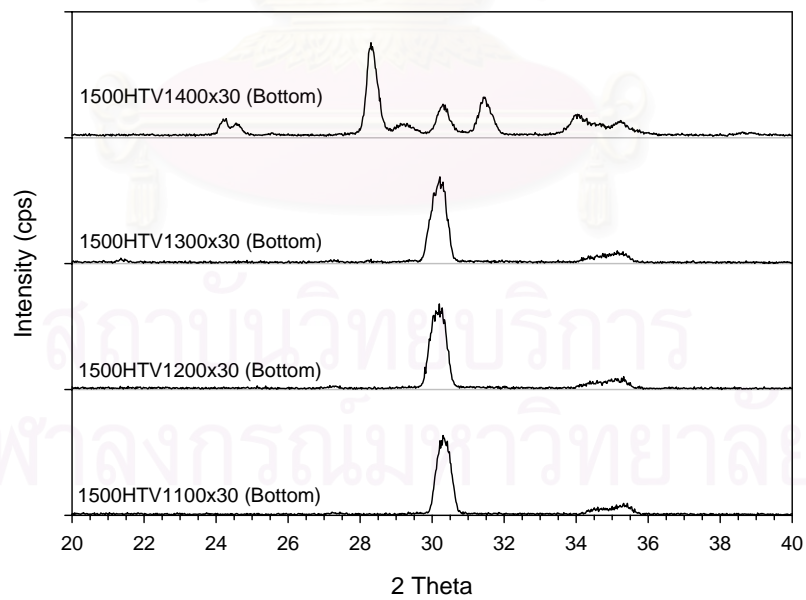
Specimen sintered at 1450°C and
annealed at 1100-1400°C for 30 min in vacuum
(Bottom surface)



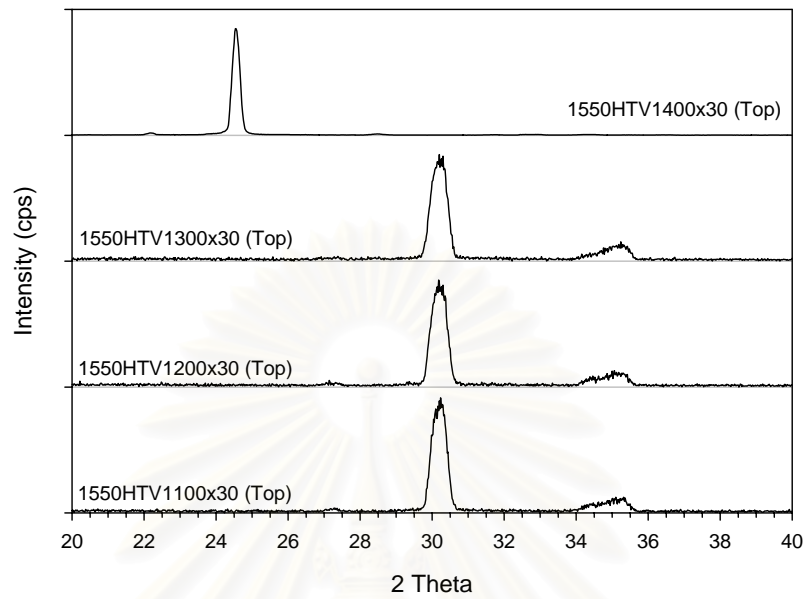
Specimen sintered at 1500°C and
annealed at 1100-1400°C for 30 min in vacuum
(Top surface)



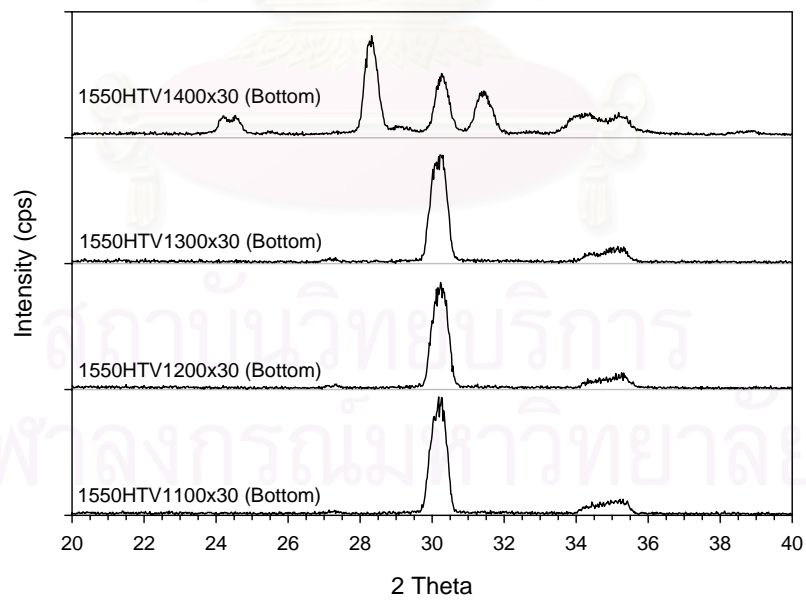
Specimen sintered at 1500°C and
annealed at 1100-1400°C for 30 min in vacuum
(Bottom surface)



Specimen sintered at 1550°C and
annealed at 1100-1400°C for 30 min in vacuum
(Top surface)



Specimen sintered at 1550°C and
annealed at 1100-1400°C for 30 min in vacuum
(Bottom surface)



Appendix 3

Weight loss of specimens sintered at 1450 and 1550°C and annealed at 1100 and 1200°C for 15 to 60 minute

HTV1100x15							
1450	Weight		% Weight Loss	1550	Weight		% Weight Loss
	Before	After			Before	After	
1	2.7188	2.7185	0.01	1	2.7803	2.7800	0.01
2	2.7300	2.7296	0.01	2	2.7515	2.7515	0.00
3	2.7520	2.7519	0.00	3	2.8056	2.8055	0.00
4	2.7410	2.7408	0.01	4	2.7939	2.7936	0.01
5	2.7542	2.7541	0.00	5	2.7954	2.7954	0.00
Average			0.01	Average			0.01
SD			0.00	SD			0.01
HTV1100x30							
1450	Weight		% Weight Loss	1550	Weight		% Weight Loss
	Before	After			Before	After	
1	2.6619	2.6611	0.03	1	2.7220	2.7218	0.01
2	2.6521	2.6516	0.02	2	2.7314	2.7315	0.00
3	2.5370	2.5362	0.03	3	2.7911	2.7911	0.00
4	2.6013	2.6007	0.02	4	2.8076	2.8076	0.00
5	2.6168	2.6166	0.01	5	2.7359	2.7359	0.00
Average			0.02	Average			0.00
SD			0.01	SD			0.00
HTV1100x60							
1450	Weight		% Weight Loss	1550	Weight		% Weight Loss
	Before	After			Before	After	
1	2.7351	2.7350	0.00	1	2.7877	2.7877	0.00
2	2.5747	2.5730	0.07	2	2.7983	2.7983	0.00
3	2.7422	2.7420	0.01	3	2.7637	2.7636	0.00
4	2.7103	2.7099	0.01	4	2.8416	2.8416	0.00
5	2.7509	2.7505	0.01	5	2.7884	2.7883	0.00
Average			0.02	Average			0.00
SD			0.03	SD			0.00

HTV1200x15							
1450	Weight		% Weight Loss	1550	Weight		% Weight Loss
	Before	After			Before	After	
1	2.7726	2.7723	0.01	1	2.7858	2.7858	0.00
2	2.7128	2.7126	0.01	2	2.7622	2.7622	0.00
3	2.7477	2.7476	0.00	3	2.7709	2.7708	0.00
4	2.7610	2.7610	0.00	4	2.7893	2.7893	0.00
5	2.7239	2.7239	0.00	5	2.7170	2.7170	0.00
Average			0.00	Average			0.00
SD			0.00	SD			0.00
HTV1200x30							
1450	Weight		% Weight Loss	1550	Weight		% Weight Loss
	Before	After			Before	After	
1	2.6730	2.6726	0.01	1	2.7108	2.7108	0.00
2	2.7013	2.7012	0.00	2	2.7736	2.7733	0.01
3	2.6748	2.6743	0.02	3	2.8128	2.8127	0.00
4	2.7129	2.7128	0.00	4	2.7946	2.7944	0.01
5	2.7031	2.7025	0.02	5	2.8252	2.8249	0.01
Average			0.01	Average			0.01
SD			0.01	SD			0.00
HTV1200x60							
1450	Weight		% Weight Loss	1550	Weight		% Weight Loss
	Before	After			Before	After	
1	2.6730	2.6726	0.01	1	2.7108	2.7108	0.00
2	2.7013	2.7012	0.00	2	2.7736	2.7733	0.01
3	2.6748	2.6743	0.02	3	2.8128	2.8127	0.00
4	2.7129	2.7128	0.00	4	2.7946	2.7944	0.01
5	2.7031	2.7025	0.02	5	2.8252	2.8249	0.01
Average			0.01	Average			0.01
SD			0.01	SD			0.00

สถาบันวิทยบริการ
จุฬาลงกรณ์มหาวิทยาลัย

Appendix 4

Vickers hardness of specimens sintered at 1450 and 1550°C and annealed at 1100 and 1200°C for 15 to 60 minute

Specimen	Micron		Hv	Hardness	
	Diagonal X	Diagonal Y		Average	SD
1450-L10	145.76	146.79	8.50E+09	8.26E+09	2.23E+08
1450-L30	257.64	257.93	8.21E+09		
1450-L50	336.23	335.47	8.06E+09		
1450-HTV1100x15-L10	144.62	146.42	8.59E+09	8.55E+09	3.71E+07
1450-HTV1100x15-L30	252.93	251.98	8.56E+09		
1450-HTV1100x15-L50	326.79	326.79	8.51E+09		
1450-HTV1100x30-L10	148.11	148.40	8.27E+09	8.22E+09	6.81E+07
1450-HTV1100x30-L30	257.27	257.27	8.24E+09		
1450-HTV1100x30-L50	334.15	334.15	8.14E+09		
1450-HTV1100x60-L10	145.76	145.09	8.60E+09	8.70E+09	8.64E+07
1450-HTV1100x60-L30	249.91	250.28	8.72E+09		
1450-HTV1100x60-L50	321.51	322.64	8.77E+09		
1450-HTV1200x15-L10	147.74	148.59	8.28E+09	8.56E+09	2.53E+08
1450-HTV1200x15-L30	249.25	249.25	8.78E+09		
1450-HTV1200x15-L50	324.81	325.19	8.61E+09		
1450-HTV1200x30-L10	149.43	150.09	8.11E+09	8.28E+09	1.46E+08
1450-HTV1200x30-L30	254.91	256.60	8.34E+09		
1450-HTV1200x30-L50	328.11	330.75	8.38E+09		
1450-HTV1200x60-L10	156.42	155.76	7.46E+09	8.71E+09	1.91E+08
1450-HTV1200x60-L30	252.93	251.60	8.57E+09		
1450-HTV1200x60-L50	319.53	321.79	8.84E+09		

Specimen remark:

1450-HTV1100x15-L10

1450 : Sintering temperature

HTV1100x15 : Annealing in vacuum at 1100°C for 15 min

L10 : Vickers hardness testing with loading of 10 kgf

Specimen	Micron		Hv	Hardness	
	Diagonal X	Diagonal Y		Average	SD
1550-L10	144.15	145.57	8.67E+09	8.81E+09	1.41E+08
1550-L30	245.94	247.93	8.95E+09		
1550-L50	320.75	321.51	8.82E+09		
1550-HTV1100x15-L10	146.13	146.13	8.52E+09	8.73E+09	2.03E+08
1550-HTV1100x15-L30	247.08	247.55	8.92E+09		
1550-HTV1100x15-L50	322.83	322.08	8.75E+09		
1550-HTV1100x30-L10	143.11	144.81	8.77E+09	8.81E+09	1.15E+08
1550-HTV1100x30-L30	247.64	246.32	8.94E+09		
1550-HTV1100x30-L50	322.08	323.58	8.72E+09		
1550-HTV1100x60-L10	161.79	162.08	6.94E+09	8.71E+09	9.55E+07
1550-HTV1100x60-L30	248.96	249.62	8.78E+09		
1550-HTV1100x60-L50	324.53	324.15	8.64E+09		
1550-HTV1200x15-L10	144.72	146.23	8.59E+09	8.88E+09	2.53E+08
1550-HTV1200x15-L30	245.28	244.91	9.08E+09		
1550-HTV1200x15-L50	317.55	319.81	8.95E+09		
1550-HTV1200x30-L10	140.76	143.40	9.01E+09	9.06E+09	7.62E+07
1550-HTV1200x30-L30	242.93	246.32	9.12E+09		
1550-HTV1200x30-L50	408.87	408.87	5.44E+09		
1550-HTV1200x60-L10	150.09	151.13	8.02E+09	8.50E+09	4.24E+08
1550-HTV1200x60-L30	248.96	252.55	8.68E+09		
1550-HTV1200x60-L50	321.32	321.32	8.81E+09		

Specimen remark:

1550-HTV1100x15-L10

1550 : Sintering temperature

HTV1100x15 : Annealing in vacuum at 1100°C for 15 min

L10 : Vickers hardness testing with loading of 10 kgf

สถาบันวิทยบริการ
จุฬาลงกรณ์มหาวิทยาลัย

Appendix 5

Bending strength of specimens sintered at 1450 and 1550°C and annealed at 1100 and 1200°C for 15 to 60 minute

Sinter	Bending Strength				
	1450	1550			
1	462.458	548.308			
2	425.066	594.114			
3	469.539	588.461			
4	505.117	479.131			
5	521.953	563.740			
Average	476.827	554.751			
SD	37.998	46.170			
HTV1100x15	Bending Strength		HTV1200x15	Bending Strength	
	1450	1550		1450	1550
1	496.322	551.271	1	605.466	607.842
2	418.102	532.114	2	525.972	613.217
3	479.755	546.482	3	574.230	632.791
4	468.853	575.208	4	565.054	607.483
5	488.474	565.147	5	545.068	587.925
Average	470.301	554.044	Average	563.158	609.852
SD	30.917	16.711	SD	30.109	16.031
HTV1100x30	Bending Strength		HTV1200x30	Bending Strength	
	1450	1550		1450	1550
1	428.677	397.418	1	528.221	545.111
2	430.736	513.499	2	508.695	513.731
3	373.640	542.211	3	460.575	471.475
4	451.608	353.973	4	469.675	552.209
5	441.278	461.810	5	460.851	638.430
Average	425.188	453.782	Average	485.603	544.191
SD	30.237	78.404	SD	30.993	61.566
HTV1100x60	Bending Strength		HTV1200x60	Bending Strength	
	1450	1550		1450	1550
1	440.123	536.661	1	587.617	623.939
2	427.391	561.733	2	542.068	641.981
3	434.237	519.150	3	605.711	621.980
4	425.736	615.672	4	569.876	594.220
5	482.534	562.035	5	480.375	623.550
Average	442.004	559.050	Average	557.129	621.134
SD	23.371	36.454	SD	48.914	17.127

BIOGRAPHY

Mr. Previt Nunthasunti was born on the 15th of February 1981, in Bangkok. After graduating with a Bachelor's degree in Materials Science (Ceramics) from the Department of Materials Science, Faculty of Science, Chulalongkorn University in 2002. He continued a further study for a Master's degree in the field of Ceramic Technology and graduated in December 2004.



สถาบันวิทยบริการ
จุฬาลงกรณ์มหาวิทยาลัย